To the Graduate Council:

I am submitting herewith a thesis written by Daniel G. Brown entitled "Compatibility of Infrared Band Models with Particulate Scattering." I have examined the final copy of this thesis for form and content and recommend that it be accepted in partial fulfillment of the requirements for the degree of Master of Science, with a major in Mechanical Engineering.

Carroll E. Peters

Dr. Carroll Peters, Major Professor

We have read this thesis and recommend its acceptance:

Roy J. Schultz

Ramson

Accepted for the Council:

Lew Minkel

Associate Vice Chancellor
and Dean of The Graduate School

STATEMENT OF PERMISSION TO USE

In presenting this thesis in partial fulfillment of the requirement for a Master's Degree at the University of Tennessee, Knoxville. I agree that the Library shall make it available to borrowers under rules of the Library. Brief quotations from this thesis are allowable without special permission, provided that accurate acknowledgment of the source is made.

Permission for extensive quotation from or reproduction of these may be granted by my major professor, or in his absence, by the Head of Interlibrary Services when, in the opinion of either, the proposed use of the material is for scholarly purposes. Any copying or use of the material in this thesis for financial gain shall not be allowed without my written permission.

Signature Daniel D. Bram

Date December 1, 1993

# COMPATABILITY OF INFRARED BAND MODELS WITH PARTICULATE SCATTERING

A Thesis

Presented for the

Master of Science

Degree

The University of Tennessee, Knoxville

Daniel G. Brown

December 1993

## ACKNOWLEDGEMENTS

I would like to thank Dr. Robert Reed for suggesting this topic and for his guidance and patience throughout the preparation of this thesis. I also express my appreciation to my major professor, Dr. Carroll Peters, for his guidance and effort; and to committee members, Dr. Arthur Mason and Dr. Roy Schultz, for their time and comments on this work.

## ABSTRACT

The prediction of the radiative heat emission from a gaseous medium which contains emitting and scattering particles has been a subject of much investigation. An example of one such problem is the calculation of the heat transfer from the exhaust of a solid propellant rocket motor to the vehicle base. Engineering approximations for the case of a purely absorbing medium have been in existence for a number of years and have withstood the test of time. One such approximation which has received much attention is called a "band model". A band model replaces the intricate emission spectra produced by a gaseous medium with essentially a bar chart representation of the spectrum; the width of each bar represents the spectral resolution of the band model, and the height of the bar represents the average value of the emission over the spectral width of the bar. Band models have many advantages in that they are based on solid physics, they provide a good representation of the real emission spectra, and computing a band model emission spectrum is relatively fast, compared to computing the true line-by-line spectrum. It is desired to exploit the band model formulation for problems with radiation scattering, such as the base heating problem mentioned previously. Upon the introduction of scattering particles to a gaseous medium, however, the band model formulation no longer applies. What was once a one-dimensional problem becomes a three-dimensional problem. Many useful mathematical approximations have been proposed to force the scattering problem into a band model type solution. These approximations retain the efficiency of the gaseous band model, however their mathematical and physical accuracy for a particular application is often unknown. The purpose of this thesis is to formulate a method by which a mathematically correct, albeit computationally slow, solution to the band model scattering

problem can be generated. These mathematically correct solutions can then be used to evaluate the accuracy of various mathematical approximations applied to the scattering problem. Three approximate treatments for which an exact band model treatment is compared are the "hybrid" band model, the two-flux scattering model, and the emission averaging treatment for the case of unequal gas and particle temperatures. For the test case examined herein, the hybrid band model approximation led to an overprediction of the emission by as much as 50% in strong gaseous absorption bands, such as the 2.7-$\mu$m water band, and displays a non-physical curve of growth. The two flux approximation performs well in strong gaseous absorption bands but overpredicts the emission in the weak gaseous emission spectral regions. Emission averaging led to an underprediction of the emission of the test case by no more than 7%.

TABLE OF CONTENTS

# LIST OF TABLES

## LIST OF FIGURES

FIGURE PAGE

# NOMENCLATURE

| | |
|---|---|
| a | absorber amount |
| b | scattering asymmetry parameter |
| d | average line spacing |
| f | probability function |
| I | radiance |
| $I_b$ | Planck black body function |
| $I_0$,$I_1$ | modified Bessel functions |
| $k$ | gas absorption coefficient |
| N | number of lines |
| P | probability function |
| S | line strength |
| $S$ | radiation source function |
| s | distance |
| T | temperature |
| u | optical path |
| W | equivalent width |

Greek Symbols

| | |
|---|---|
| $\alpha$ | absorptivity |
| $\beta$ | total extinction cross-section |
| $\theta$ | scattering angle |
| $\Omega$ | direction of radiation propagation |
| $\omega$ | albedo |
| $\sigma$ | particle cross-section |
| $\sigma_\varepsilon$ | emissivity standard deviation |
| $\tau$ | transmission |
| $\varepsilon$ | emission |
| $\gamma$ | line half width |
| $\Gamma$ | particle absorption fraction |
| $\nu$ | wavenumber |

Subscripts

| | |
|---|---|
| a | absorption |
| e | extinction cross-section |
| g | gas |
| p | particle |
| s | scattering |
| sl | single line |
| $\upsilon$ | monochromatic |

Other

| | |
|---|---|
| $\overline{(\ )}$ | denotes spectral average |

# 1.0 INTRODUCTION

This thesis concerns the engineering approximations used to treat the problem of the emission of radiation from a region which contains a spatial distribution of gaseous, liquid and solid constituents. One is forced to use various approximate treatments in radiative heat transfer calculations due both to the inadequate knowledge of the physical parameters of the problem and due to the computational complexity that a rigorous treatment of all of the physics of the problem would present. Engineering approximations for the radiative energy transfer from a gaseous medium have been in existence for several decades. One of the more rigorous approaches to this problem has been given the descriptive title "band model".[1] In a band model, the monochromatic nature of the emission spectra of a radiating gas is replaced by a spectra consisting of bands of finite spectral width, hence the problem is transformed from one of infinite spectral resolution to one of a much coarser spectral resolution. For the gas-only emission problem and for most applications, these band models do provide a satisfactory representation of the underlying physics of the problem. An efficient approximation to extend this theory to model a medium which contains both emitting and scattering particles has only been partially successful and is still ongoing[2] Because of the three-dimensionality introduced by the scattering particles, band model theory no longer directly applies; additional terms appear in the governing transport equation which are not taken into account in the traditional band model formulation. Therefore, additional approximations must be made to make the scattering problem amenable to a band model solution. A necessary part of this search for a sufficiently accurate band approximation to the scattering problem is the ability to generate band averaged solutions to the scattering problem (the governing transport

equation) which are mathematically correct. Then the problem can be attacked with the approximations and the applicability of the approximation for the particular physical situation under investigation can be assessed.

## 2.0 THE BAND MODEL/SCATTERING INCOMPATIBILITY

The gaseous band model/scattering incompatibility will be demonstrated with a simple example. The detailed development and discussion of the solution techniques applied to this example problem will be deferred until subsequent sections.

The radiative energy emission of a combustion exhaust region which contains both gaseous and particulate species is to be computed. At the present time, the detailed line parameter database needed to compute the line emission spectra for a high temperature gas, consisting of complex molecules like $H_2O$ and $CO_2$ for instance, does not exist. This is due to the difficulties of measuring high resolution spectra of these species at elevated temperatures to assist in the prediction of line parameters. Indeed, for heat transfer calculations, such a high degree of modeling fidelity and computational expense may not be warranted. Therefore, an alternative prediction procedure, called a band model, is often used to approximate the monochromatic emission spectra. The band model replaces the true monochromatic emission spectra with one of finite spectral resolution. With this approach, only spectral averages of the molecular line parameters are required to produce the band model spectra. The spectrally averaged line parameters, or band model parameters, for gas temperatures typical of combustion products are measurable and have been available for several years.

For the moment, scattering particles are ignored and the gas-only emission spectra is computed for an example problem. For the no-scattering problem, the calculation involves a one-dimensional integration along the observation line of sight through the gas. The monochromatic emission spectra of the gas and its band model approximation are shown in Figure 1. This spectra was computed using line data from the High Resolution

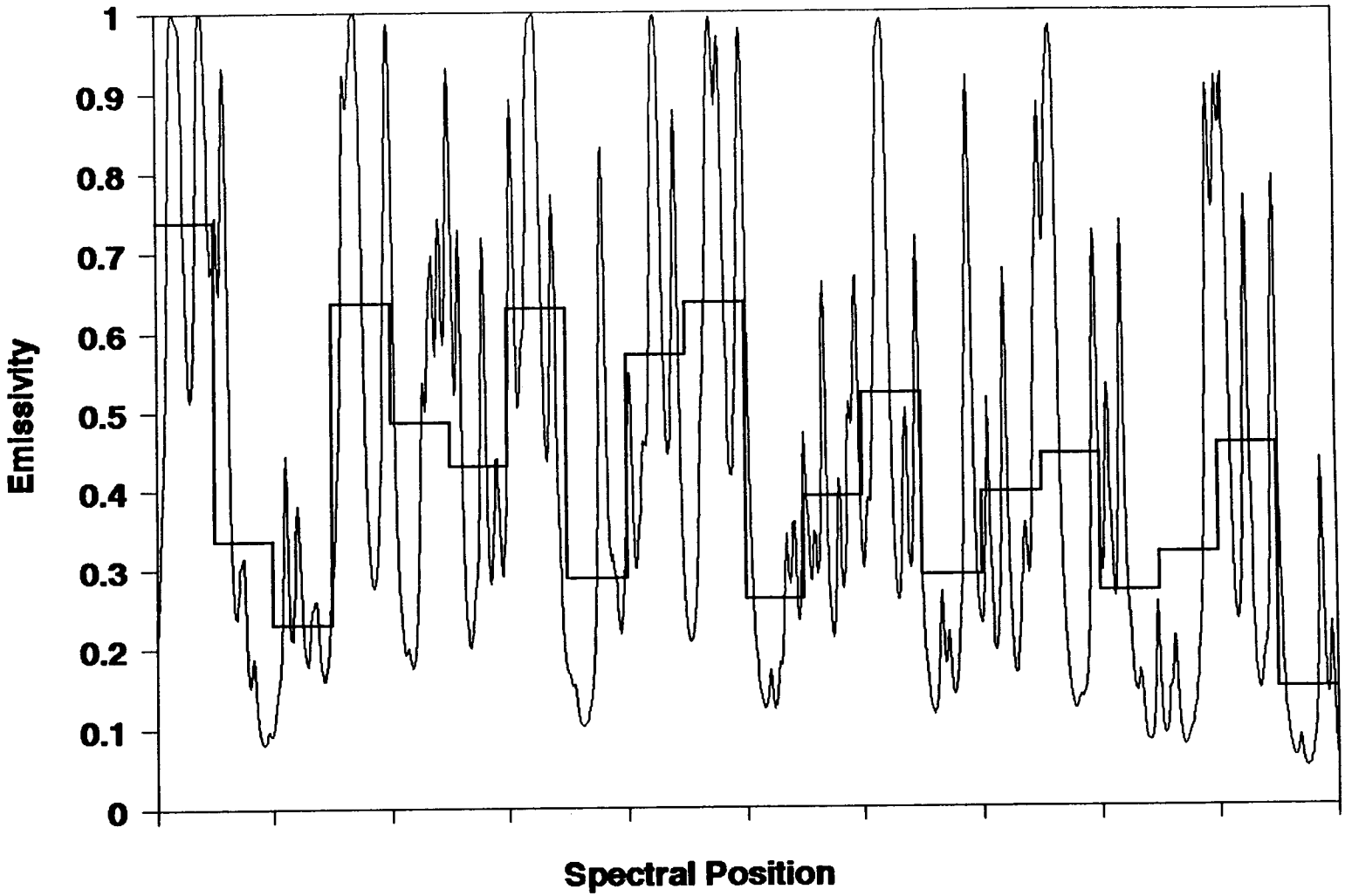


Figure 1. Gas Only Monochromatic and Band Emission Spectra.

line data base (HITRAN)[3] with a simple FORTRAN program. The HITRAN line parameter data base is adequate for temperatures typical of atmospheric gas paths, however it is incomplete for applications involving temperatures typical of combustion and is used here purely for illustrative purposes. One sees from Figure 1 that the band model represents the average of the monochromatic emission spectra over small frequency intervals. The step function format is used for the band calculation to emphasize the spectral band-average nature of the solution.

When scattering particles are added to the example problem, the energy transport equation becomes three dimensional and an integration over the entire emitting volume must be performed. To determine the emission, ε, for the case with scattering, one is forced to use a band model solution for computational efficiency and because of the absence of line data at the high temperatures of interest. A rigorous band model approach to the scattering problem has not been performed until now. Instead, an approximate scattering band model approach has been used which performs the correct spectral average for the unscattered emission component, however the scattered emission component is evaluated with the band averaged line parameters. That is:

$$\bar{\varepsilon} = \bar{\varepsilon}_{uns}(k) + \varepsilon_{scat}(\bar{k}) \tag{2.1}$$

instead of the mathematically correct formulation:

$$\bar{\varepsilon} = \bar{\varepsilon}_{uns}(k) + \bar{\varepsilon}_{scat}(k) \tag{2.2}$$

where the overbar represent spectral band averages, $k$ is the gaseous absorption coefficient and the subscripts "uns" and "scat" represent the unscattered and scattered components of the emission, respectively. Thus the band model/scattering incompatibility involves an incorrect spectral averaging of the scattered emission components (Equation (2.1)).

The three dimensional, monochromatic solution for the example gas with scattering particles is shown in Figure 2. The method used to obtain this solution will be discussed in Section 7. The mathematically correct band solution can be formed by either band averaging the monochromatic solution shown in Figure 2, or by tracking the scattered and unscattered components in the solution technique and applying Equation (2.2). These two approaches are equivalent. The incorrect scattering band model solution is formed by using Equation (2.1). The comparison between these two approaches and the spectral emission is shown in Figure 2. The spectral emission of the emitting/scattering medium is shown on Figure 2 as the rapidly varying curve. The two band solutions are shown with a step function format to emphasize the band nature of the solution. The mathematically correct band solution is shown as the solid step function curve and is the average value of the monochromatic emission curve at the resolution of the band model. This is the solution obtained using Equation (2.2). The step function curve represented by dashed line is the band solution to the scattering problem which is given by Equation (2.1) which contains an incorrect spectral averaging of the scattered terms. The two band solutions are different, and the band model/scattering incompatibility is illustrated.

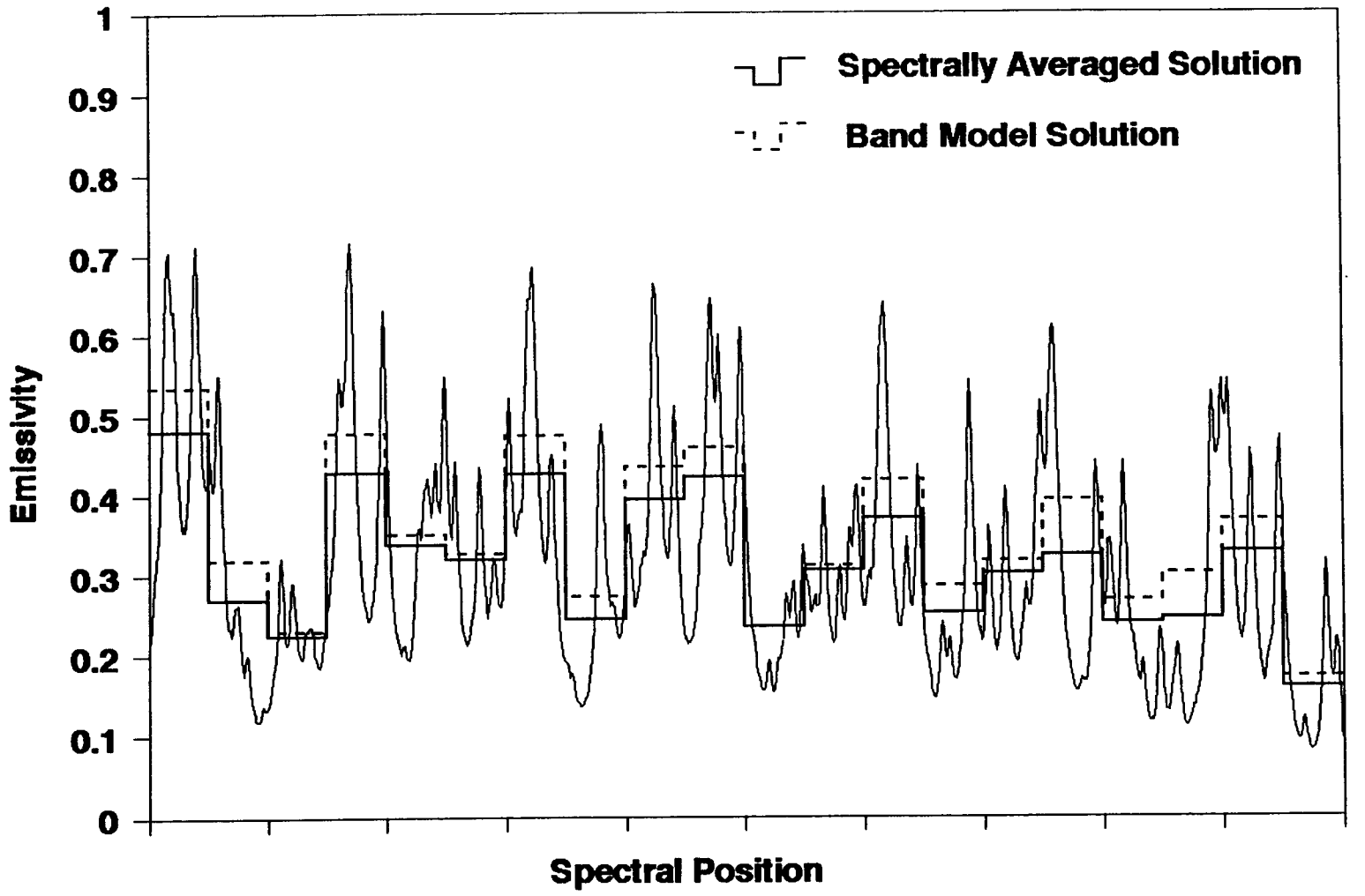


Figure 2. Monochromatic and Band Averaged Scattering Solutions.

# 3.0 ROCKET MOTOR EXHAUSTS

The combustion products from typical rocket motors exit the vehicle in the form of a high-temperature, high-mass-flux gas stream which often contains solid and/or liquid phase combustion products. A schematic of the typical base heating scenario is shown in Figure 3. Due to the proximity of the exhaust gas and the rocket vehicle, heating of the body by the exhaust gas will certainly occur, and in some cases the vehicle temperature may increase enough to damage the vehicle. The amount of radiative heating is dependent upon several parameters including the spatial distribution of temperature, pressure and species concentration within the exhaust, as well as the geometry of the exhaust/vehicle view. The presence of solid particles in the exhausts of many rocket motors changes the emission of the medium and introduces radiation scattering. Unfortunately for most base heating problems, the lines of sight from the vehicle to the plume travel through relatively long paths in the exhaust gas, as shown in Figure 3, and therefore may result in high heat flux to the body. Some lines of sight, however, may pass through relatively short exhaust paths which requires that the prediction technique used for heat transfer calculations perform correctly for both optically "thick" and optically "thin" paths.

Most of the rockets in use today are typically fueled with either liquid or solid propellants.[4,5] In a liquid-propellant rocket motor, the fuel and oxidizer are injected into the combustion chamber in the liquid phase. For moderate and low thrust rocket motors this is usually accomplished by a pressurized system in which the propellant storage tanks are pressurized to the proper pressure to achieve the desired fuel and oxidizer flow rates and combustion chamber pressure. Almost all launch system liquid propellant engines, most notably the Space Shuttle Main Engine, are pump fed. Here the propellant feed

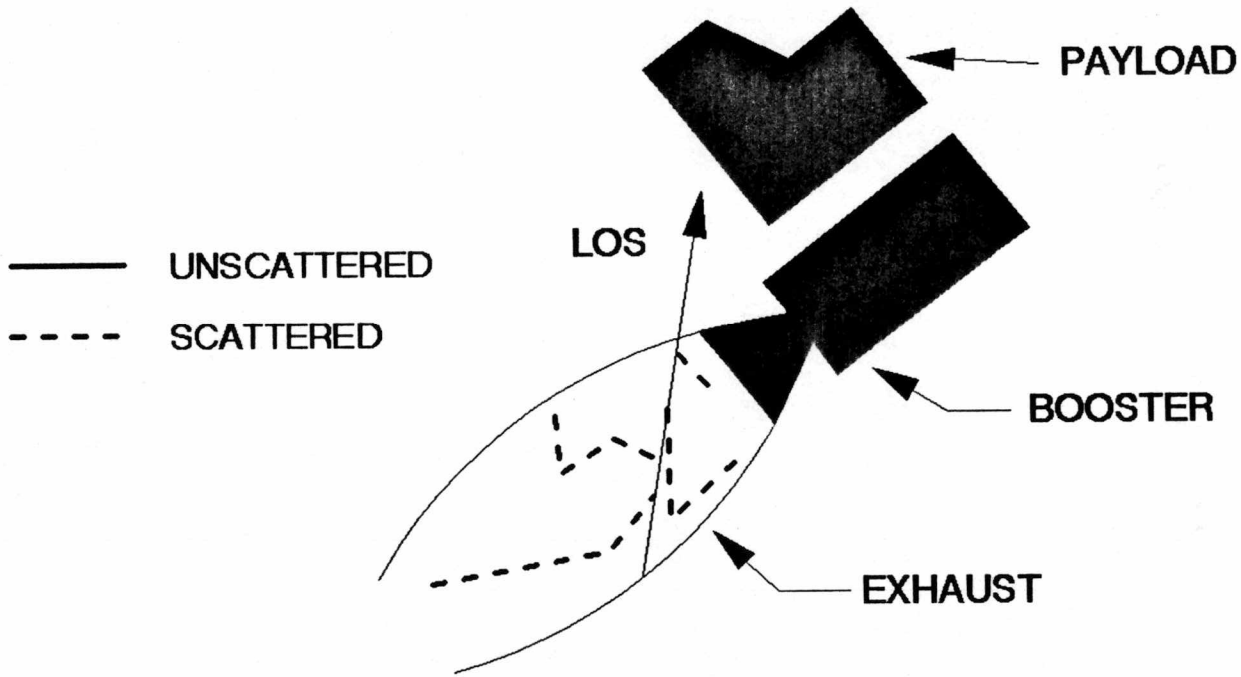


Figure 3. Base Heating Scenario.

system is driven by turbopumps which are powered by partial combustion of the fuel. The task of a liquid propellant rocket combustion chamber is to adequately mix the fuel and oxidizer, and to provide a suitable volume for the associated energy release. The bell shaped converging diverging nozzle provides the most efficient contour for converting the high pressure fluid in the combustion chamber into a high velocity fluid at the nozzle exit for a rocket engine.[6] The constituents present in the exhaust plume of liquid propellant rocket engines most important for heat transfer analysis are gaseous $H_2O$, $CO_2$, CO and in some cases sub-micron-diameter carbon-particle agglomerates.

Solid rocket motor propellants are usually contained entirely within the combustion chamber or case. The solid propellant, or grain, is either a chemical or a mechanical mixture of all of the constituents necessary for combustion. Metals, such as aluminum, are often included in the propellant formulation to increase the energy release of the combustion process, and to provide a stability mechanism in the combustion chamber. Propellant formulations with aluminum loadings of up to 15% by mass are common. Various grain configurations are used depending on the desired thrust profile characteristics. The combustion products are accelerated through a converging diverging nozzle and ejected from the nozzle exit. For the case of an aluminized propellant that produces an exhaust flow containing solid particles, conical nozzles are often used in order to minimize particle impingement on the nozzle walls. The typical gaseous species present in the exhaust of a solid rocket motor that are important for heat transfer analysis are gaseous $H_2O$, $CO_2$, CO and HCl. In the rocket exhaust, the metals in the propellant grain show up as metal oxide particles in the liquid and/or solid phase, depending on the local gas temperature and the history of the particles through the nozzle. Particle sizes are on the order of 1 to 10-$\mu$m. The physical characteristics of the solid and liquid particles have a large effect on the heat radiated by the motor exhaust.

# 4.0 HEAT TRANSFER

When two objects within a system are allowed to interact, an energy exchange occurs. If the objects are in thermal equilibrium, the net energy exchange is zero. When the objects are characterized by different temperatures, a net flow of energy (heat), will occur in order to bring the objects into equilibrium. Energy transport between objects is often classified by three mechanisms; conduction, convection and radiation. The mechanism responsible for conduction and convection heat transfer is the transfer of energy due to collisions of the molecules of the two systems. Heat transfer by radiation involves the emission and subsequent absorption of electromagnetic energy (photons) by the molecules comprising the systems.

## 4.1 Radiation Heat Transfer

Radiation heat transfer involves the transport of energy between two systems in the form of electromagnetic waves.[7] For a system in thermal equilibrium, the emission is characterized by the temperature of the system. The mechanism which gives rise to radiative heat transfer involves the interaction of electromagnetic waves and the molecules comprising the system. Electromagnetic waves are emitted from a molecule as a result of changes in the energy of the molecule from a higher energy state to a lower energy state. The energy of the emitted wave packet, or photon, is equivalent to the energy lost by the molecule. Within a system in thermodynamic equilibrium, as a molecule looses energy from the emission of electromagnetic waves, an equivalent amount of energy is being absorbed by the molecule as a result of absorption of electromagnetic waves from other

molecules in the system. When two systems of unequal temperatures are allowed to interact by radiative heat transfer, energy is transferred by both systems, though a net flow of energy exists from the high energy (temperature) system to the low energy (temperature) system.

### 4.1.1 Radiation from Solid Surfaces

Radiation emission from solids is characterized by a continuum of energy states. When a beam of monochromatic radiation is absorbed by the solid, a resultant temperature increase of the body occurs. This temperature increase leads to an increase in emission from the solid, and the radiated energy is in the form of a continuous spectra due to the presence of a continuum of energy states in the solid. An ideal emitter is termed a black body because theoretically the body absorbs all incident radiation. Thus if one were to illuminate the black body, it would still appear black because all incident photons would be absorbed, and none reflected from the surface for detection. Owing to its perfect absorptivity, the black body is also a perfect emitter since for a body in thermal equilibrium, the spectral absorptivity and emissivity are equal which is stated by Kirchoff's law. Emission from a black body is governed by the Planck black body equation.

### 4.1.2 Radiation from Gases

For most practical temperatures and pressures, gases absorb and emit energy at discrete frequencies (energies) as opposed to radiative transfer from solid surfaces which emit and absorb as a energy continuum. A gas molecule interacts with a incoming photon only under certain conditions. The energy possessed by the incident photon must be

absorbed by the molecule and the energy must be of magnitude to raise the molecule to a higher energy level, thus increasing the energy of the molecule. The fraction of the incident energy that is absorbed by the gas per unit length along the path of the radiation beam is characterized by the monochromatic absorption coefficient, $k_\nu$.

### 4.1.3 Radiation Absorption and Scattering by a Particle

Upon interaction with a particle, a photon may either be absorbed or scattered. The ratio of the rate of energy scattered by the particle to the incident energy flux is called the particle scattering cross-section. The particle absorption cross-section is defined as the ratio of the rate that energy is absorbed to the incident energy flux. If the photon is scattered, its energy is conserved but its direction of propagation may be changed depending on the characteristics of the photon and the particle. The scattering angle is defined as the angle between the incident and scattered directions. Two scattering theories which describe the direction of the scattered photon are the theories of Rayleigh and Mie.[8] Rayleigh scattering theory applies when the wavelength of the incident radiation is much larger than the diameter of the spherical scattering particles. Mie theory is general and is applicable when the radiation wavelength and the particle diameter are approximately equivalent. The scattering phase function describes the directional distribution of the scattered radiation. The scattering phase function predicted by Rayleigh theory for unpolarized light can be expressed in closed form as is given by:

$$P(\Omega' \bullet \Omega) = \frac{3}{4}(1 + COS^2\theta)$$

where

$P(\Omega' \bullet \Omega)$ is the probability that a photon traveling in the $\Omega'$ direction is scattered into the $\Omega$ direction

$\theta$ is the angle between $\Omega$ and $\Omega'$, the scattering angle

The scattering phase function predicted by the Mie theory cannot be expressed in closed form but is often approximated by the Henyey-Greenstein function which provides an acceptable degree of approximation of the Mie scattering function for many applications. Representative scattering phase functions for the Rayleigh and Henyey-Greenstein approximation to the Mie theory are shown in Figure 4. The one free parameter in the Henyey-Greenstein phase function is the backscatter fraction, b, which is interpreted as the average value of the cosine of the scattering angle. A backscatter fraction of 1 represents complete backward scattering (scattering angle = 180°) while b=0 implies isotropic scattering.

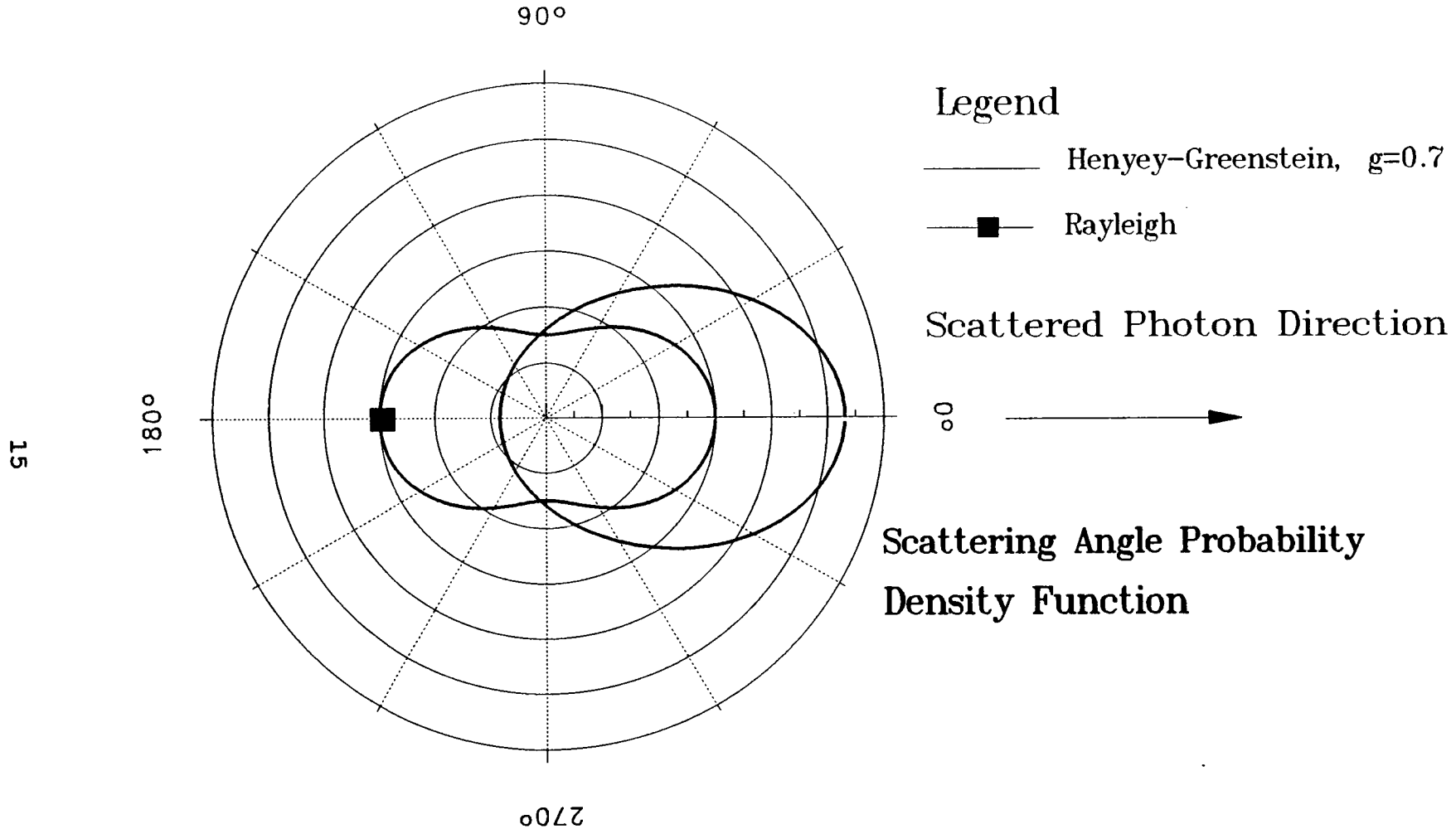


Figure 4. Two Common Scattering Phase Functions.

## 5.0 THE RADIATIVE TRANSPORT EQUATION

The equation of radiative energy transport can be derived using various approaches. The approach taken here is to apply the conservation of energy to an elemental volume along the path of a monochromatic beam of radiation.[7] This elemental volume is shown in Figure 5. The direction of energy transport is along the +s axis. A beam of monochromatic radiation enters the volume at s; the beam exits at (s+$\delta$s). The intensity may be augmented within this volume by emission of photons within the volume, and by scattering of radiation from other directions into the direction of beam propagation. These gain terms are called the source function and are written as:

$$S_\nu(s) \equiv (1-\omega_\nu) I_{b\nu}(T) + \omega_\nu \int_{4\pi} P(\Omega' \bullet \Omega) I_\nu(s,\Omega') d\Omega' \tag{5.1}$$

where

$$\omega_\nu \equiv \frac{\sigma_{s_\nu}(s)}{\beta_\nu(s)} \text{, the albedo} \tag{5.2}$$

$\beta_\nu(s) = k_\nu(s) + \sigma_{e_\nu}(s)$ , the total extinction cross-section of the path

$\sigma_{e_\nu}(s) = \sigma_{s_\nu}(s) + \sigma_{a_\nu}(s)$, the particle extinction cross-section

$I_{b\nu}(T)$, the Planck black body function

The first term on the right-hand side of Equation (5.1) represents the emission gain along the line of sight due to the emission within the control volume. The second term represents the gain due to radiation which enters the control volume from all directions and is scattered into the line of sight direction due to scattering within the control volume. The beam may be attenuated by absorption and scattering by the particles within the volume. This loss term is written as :

$$\beta_\nu(s) I_\nu(s,\Omega)$$

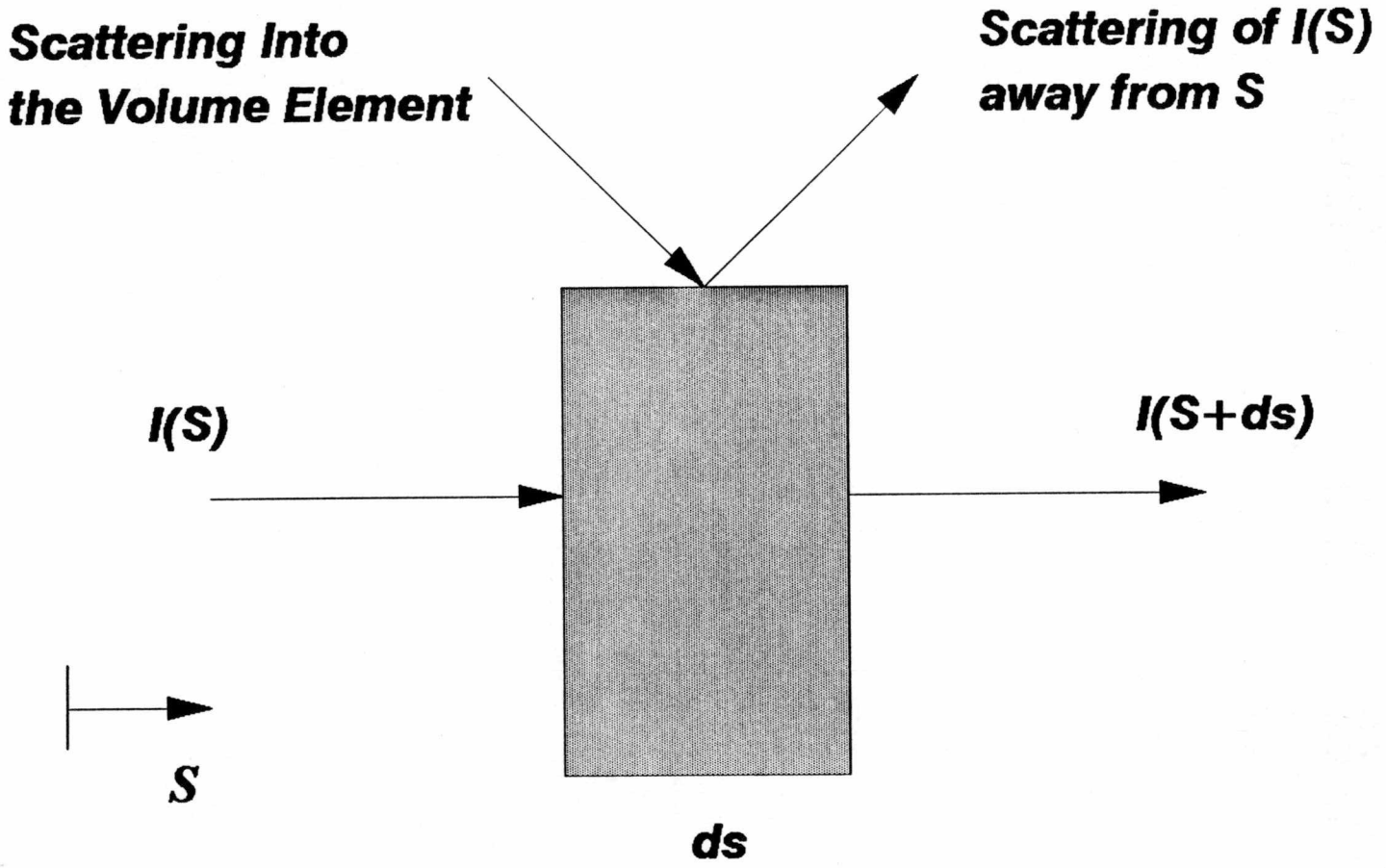


Figure 5. Elemental Volume for Derivation of Transport Equation.

The governing equation for radiative transport is:[7]

$$\frac{1}{\beta_\nu(s)}\frac{\partial I_\nu(s,\Omega)}{\partial s}+I_\nu(s,\Omega)=S_\nu(s) \tag{5.3}$$

The formal solution of this equation is:[7]

$$I_\nu(s,\Omega)=I_{b\nu}(s_0)\exp\left[-\int_{s_0}^{s}\beta_\nu(s')ds'\right]+\int_{s_0}^{s}\beta_\nu(s')S_\nu(s',\Omega)\exp\left[-\int_{s'}^{s}\beta_\nu(s'')ds''\right]ds' \tag{5.4}$$

Equation (5.4) relates the radiance along a given line of sight from $S_0$ to S to the radiative properties along the line of sight connecting $S_0$ and S and the incident radiation at $S_0$. No general solution for the radiance can be obtained from this equation because of its dependence on the source function, which is not known a priori.

## 5.1 Spectrally Averaged Solution

If a spectrally averaged solution is desired, Equation (5.4) must be averaged over the desired frequency interval. The averaged solution may be written as:

$$\overline{I_{\delta\nu}(s,\Omega)}=\frac{1}{\delta\nu}\int_{\delta\nu}I_\nu(s,\Omega)d\nu \tag{5.5}$$

## 5.2 Gaseous Radiative Transport

For the special case of the medium of interest being composed of absorbers only, the albedo, $\omega_\nu$, is zero and the transport equation is simplified to the familiar form:

$$\frac{1}{k_\nu(s)}\frac{\partial I_\nu(s,\Omega)}{\partial s}+I_\nu(s,\Omega)=I_{b\nu}(T) \tag{5.6}$$

which has the following solution for a zero radiance boundary condition.

$$I_\nu(s,\Omega) = \int_0^s k_\nu(s') I_{b\nu}(T) \exp\left[-\int_{s'}^s k_\nu(s'')ds''\right]ds' \tag{5.7}$$

## 5.3 Homogeneous Medium

If the gas path is homogeneous, Equation (5.7) can be integrated to obtain the transmission of the homogeneous gas path. This is referred to as Beer's Law.

$$\tau_\nu = e^{-k_\nu s} \tag{5.8}$$

# 6.0 SOLUTION TO THE RADIATIVE TRANSPORT EQUATION WITHOUT SCATTERING (BAND MODELS)

With certain assumptions, the monochromatic emission spectra of a gas may be approximated with good accuracy by a band model. For the case of a homogeneous media, Equation (5.7) may be simplified to obtain an expression for the monochromatic transmission of the media Equation (5.8). The spectral average of the transmission over a small spectral band $\delta\nu$, may be written:

$$\bar{\tau}_{\delta\nu} = \frac{1}{\delta\nu}\int_{\delta\nu} \tau_\nu d\nu = \frac{1}{\delta\nu}\int_{\delta\nu} e^{-k_\nu s} d\nu \tag{6.1}$$

Clearly, the following is true in general:

$$\bar{\tau}_{\delta\nu} \neq e^{-\bar{k}_{\delta\nu} s}$$

where

$$\bar{k}_{\delta\nu} = \int_{\delta\nu} k_\nu d\nu$$

A band model seeks to represent the spectral average of the transmission within a spectral band by a function of the band averaged line parameters, $\bar{k}_{\delta\nu}$, of the spectral lines within the band. The equivalent width of a single line, $W_{sl}$, is introduced and is interpreted as the spectral width of a totally absorbing line within the spectral interval which yields an equivalent band-averaged absorption.

$$W_{sl} = \int_0^\infty \alpha_\nu d\nu \tag{6.2}$$

where

$\alpha_\nu$ is the spectral absorptance

There are many band model formulations, each of which are related to a specific set of assumptions which are used to describe individual lines within the spectral band. These assumptions concern the line intensities or strengths, line shape, and the number and spectral distribution of the lines within the spectral band. The line intensity is defined as the frequency integral over the spectral line shape. The line shape is a result of spectral broadening of the line due primarily to Doppler (thermal) broadening, Lorentz (pressure) broadening or a combination of the two, which is called the Voigt line shape.

## 6.1 Regular Band Models

The monochromatic emission spectra of some molecules, especially diatomics, may best be approximated by a model consisting of regularly spaced lines of equal intensity and shape.[1] Two band models derived under these assumptions are the Elsasser and Golden band models for a band of regularly spaced, equal intensity lines which are pressure broadened or thermally broadened, respectively.[1] These band models are of limited use for the typical combustion products of rocket motors and will not be discussed further.

## 6.2 Random Band Models

When the lines which constitute the emission spectra are not regularly spaced, such as might be expected from a polyatomic molecule, a model where the line spacing and line strengths are described statistically is more appropriate. The random band model relates

the band averaged transmission of a number of these lines to the equivalent width of one line within the band averaged over the line strength probability distribution function. The following development for the random band model is repeated from Goody and Plass.[9,10]

The assumptions for a random band model are:

1) The lines within the spectral interval are randomly placed.
2) The lines all have the same spectral shape.
3) The strength of the lines within the spectral interval can be described statistically, and the line strength is uncorrelated with spectral position.

Let there be a spectral interval, composed of N randomly spaced lines, of width $N\delta$, where $\delta$ is the average line spacing. The line strengths of the lines within this interval are characterized by the line strength distribution function P(S). The contribution from N lines within the spectral interval, to the absorption coefficient at the frequency $\nu_0$ is given by:

$$k_{\nu_0} = \sum_{i=1}^{N} k_{\nu_i} \tag{6.3}$$

where $k_{\nu_i}$ is the absorption coefficient of the $i^{th}$ line at the spectral position $\nu_0$.

The absorption coefficient at $\nu_0$, of the line centered at $\nu_i$ is determined by the line shape function. Then from Beer's Law (Equation (5.8)), the resulting transmissivity of a gas path at the frequency $\nu_0$ due to the N lines is:

$$\tau_{\nu_0} = \exp\left[-a\sum_{i=1}^{N} k_{\nu_i}\right] = \prod_{i=1}^{N} \exp\left(-ak_{\nu_i}\right) \tag{6.4}$$

where

$a$ is the absorber amount.

For random line spacing within the spectral interval, the probability that a line lies within the spectral interval $\nu_i$ to $(\nu_i + d\nu_i)$ is $d\nu_i / \delta$ and the joint probability that there are lines in all spectral intervals $\nu_i$ to $(\nu_i + d\nu_i)$ is:

$$f(\nu_i) = \prod_{i=1}^{N} \frac{d\nu_i}{\delta} \tag{6.5}$$

Since the line position probability function is zero outside the spectral interval $\delta\nu$, the band averaged transmission can then be formed by integrating the transmission function over the line position probability function as follows:

$$\bar{\tau}_{\delta\nu} = \int_{\delta\nu} \tau_\nu f(\nu) d\nu \tag{6.6}$$

by substituting Equation (6.5) into Equation (6.6), one obtains:

$$\bar{\tau}_\nu = \frac{\int_{-\frac{1}{2}N\delta}^{\frac{1}{2}N\delta} \prod_{i=1}^{N} \exp\left(-ak_{\nu_i}\right) \frac{d\nu_i}{\delta}}{\int_{-\frac{1}{2}N\delta}^{\frac{1}{2}N\delta} \prod_{i=1}^{N} \frac{d\nu_i}{\delta}} \tag{6.7}$$

where the denominator has been included to normalize the line position probability distribution function. The products can be brought outside the integrals and the integration in the denominator can be performed to yield the following:

$$\bar{\tau}_{\delta\nu} = \left\{ \frac{1}{N} \int_{-\frac{1}{2}N\delta}^{\frac{1}{2}N\delta} \exp\left(-ak_\nu\right) \frac{d\nu}{\delta} \right\}^N \tag{6.8}$$

which can be rewritten:

$$\bar{\tau}_{\delta\nu} = \left\{ 1 - \frac{1}{N} \int_{-\frac{1}{2}N\delta}^{\frac{1}{2}N\delta} \left[ 1 - \exp\left( -ak_\nu \right) \right] \frac{d\nu}{\delta} \right\}^N \tag{6.9}$$

As the number of lines, N, within the spectral band $\delta$, goes to infinity, Equation (6.9) is recognized as an expansion for the exponential function with the exponent being product of the line strength distribution function and equivalent width of a single line within the array, or:

$$\lim_{N \to \infty} \left( 1 + \frac{\chi}{N} \right)^N = e^{\chi}$$

and

$$\bar{\tau}_{\delta\nu} = \exp\left[ -\frac{1}{\delta} \int_{-\infty}^{+\infty} \left[ 1 - \exp\left( -ak_\nu \right) \right] d\nu \right] \tag{6.10}$$

which is simply the exponential of the equivalent width (Equation(6.2)) of a single line within the spectral interval.

One commonly used random band model is the Goody model, which assumes that the emission spectra is composed of a random array of spectrally uncorrelated, Lorentz shape lines with a exponential line strength distribution. That is, the probability that a line, within the spectral interval, has a strength of S is:

$$P(S) = \frac{1}{S_o} e^{-\frac{S}{S_o}} \tag{6.11}$$

where $S_0$ is a constant. The equation of the equivalent width of a single isolated pressure broadened line is given by the Landeberg-Reiche function.[11]

$$W_{sl} = 2\pi\alpha x e^{-x}\left[I_0(x) + I_1(x)\right] \tag{6.12}$$

where

$$x = \frac{Su}{2\pi\alpha}$$

and $I_0$ and $I_1$ are modified Bessel functions.

Thus the band averaged transmission for the Goody model is given as the product of the Ladenburg-Reiche function and the exponential line strength distribution.

$$\overline{W}_{sl} = \int_{-\infty}^{+\infty} W_{sl} P(S) dS \tag{6.13}$$

This integral can be found in some integration tables.[12] The resultant band averaged absorption is given by:

$$\overline{\alpha} = 1 - \exp\left[\frac{-2\pi\left(\frac{\gamma}{d}\right)x_0}{\sqrt{1+2x_0}}\right] \tag{6.14}$$

The remaining task is to relate the parameters $S_0$, $\gamma$ and d to observable physical parameters. This can be done by forcing the band model solution to agree in the limiting cases of optically thin and thick media.[13] The exponential band model curve of growth is illustrated in Figure 6. Shown is absorption as a function of absorber amount. The optically thin limit is delineated by a linear relationship between the absorber amount and

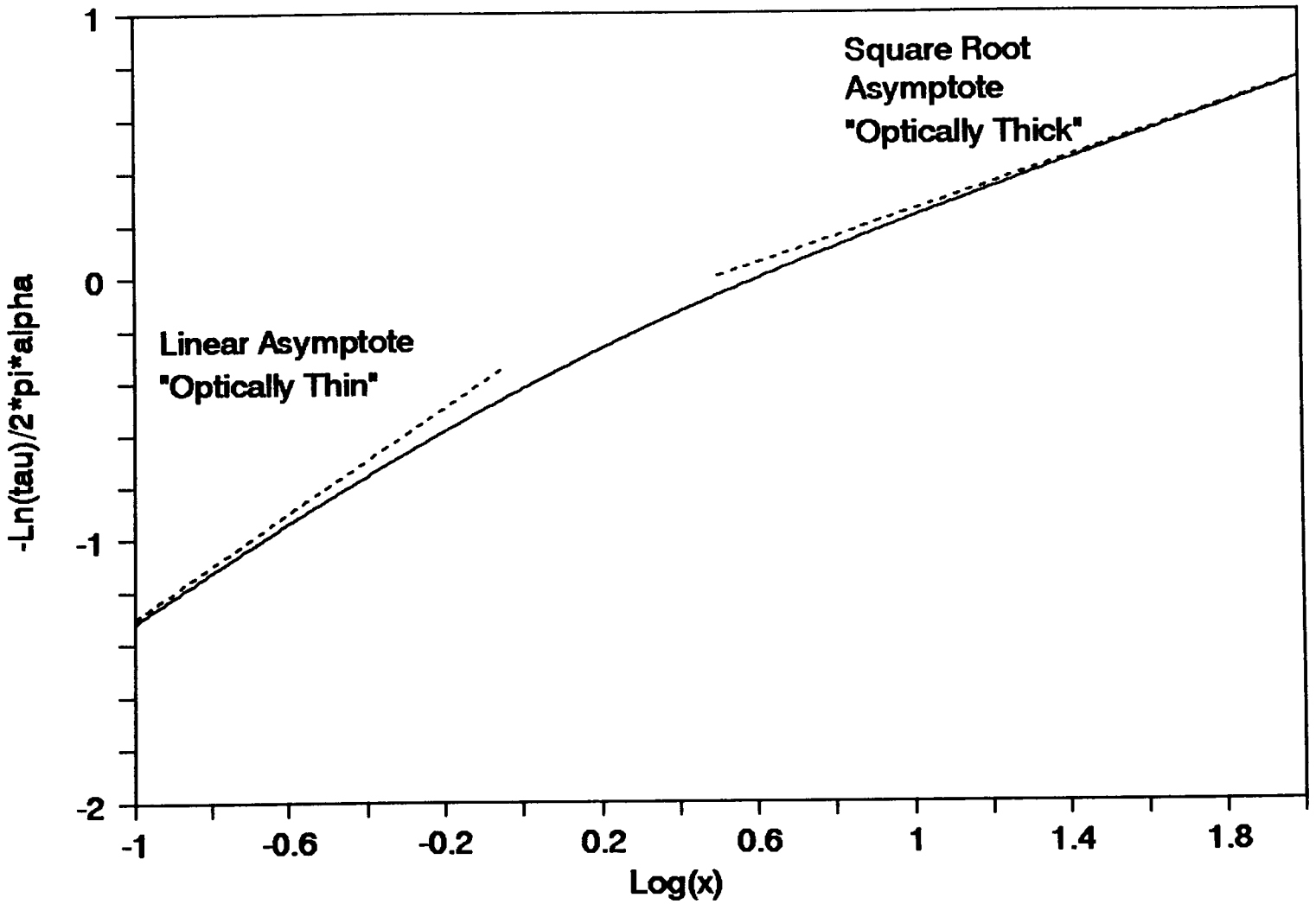


Figure 6. Exponential Band Model Curve of Growth.

absorption. The optically thick limit is characterized by a square-root dependence of absorption with absorber amount. In the linear, optically thin limit:

$$-\ln \tau \rightarrow \frac{S_0 u}{d} \qquad \text{as } u \rightarrow 0$$

and in the optically thick, square-root region:

$$-\ln \tau \rightarrow \frac{2\sqrt{S_0 \gamma u}}{d} \qquad \text{as } u \rightarrow \infty$$

Thus the band model parameters can be obtained by making transmission measurements along a gas path within these two limiting regions.

# 7.0 SOLUTION OF THE RADIATIVE TRANSPORT EQUATION WITH SCATTERING

When scattering particles are present, the full monochromatic transport equation must be solved (Equation (5.3)). Solutions to this equation can be obtained with methods such as successive approximations (Neumann series solution)[14] or with a Monte Carlo simulation.[15]

## 7.1 Monte Carlo Method as a Means of Solution

The Monte Carlo simulation procedure involves incorporating all of the relevant probabilities associated with a physical situation into a game. The game is then played a significant number of times, the outcome of each game is tabulated. After the game has been played many times, the cumulative probability of all possible outcomes can be defined. The physics of radiation heat transfer are readily expressed in terms of cumulative probabilities. If radiative heat transfer from point A to point B is thought of as photons streaming from A in the direction of B, a simplified depiction of four possible outcomes is shown in Figure 7. In their journey from A to B, some photons will be absorbed by the intervening gaseous media either without being scattered (photon 1) or after scattering (photon 2). Other photons may encounter a scattering particle and be scattered away from the direction of B (photon 3) while others may be scattered several times and still reach B from a different direction (photon 4). If one were interested in the heat transfer from the gaseous media to B, this game would have to be played many times, and for many

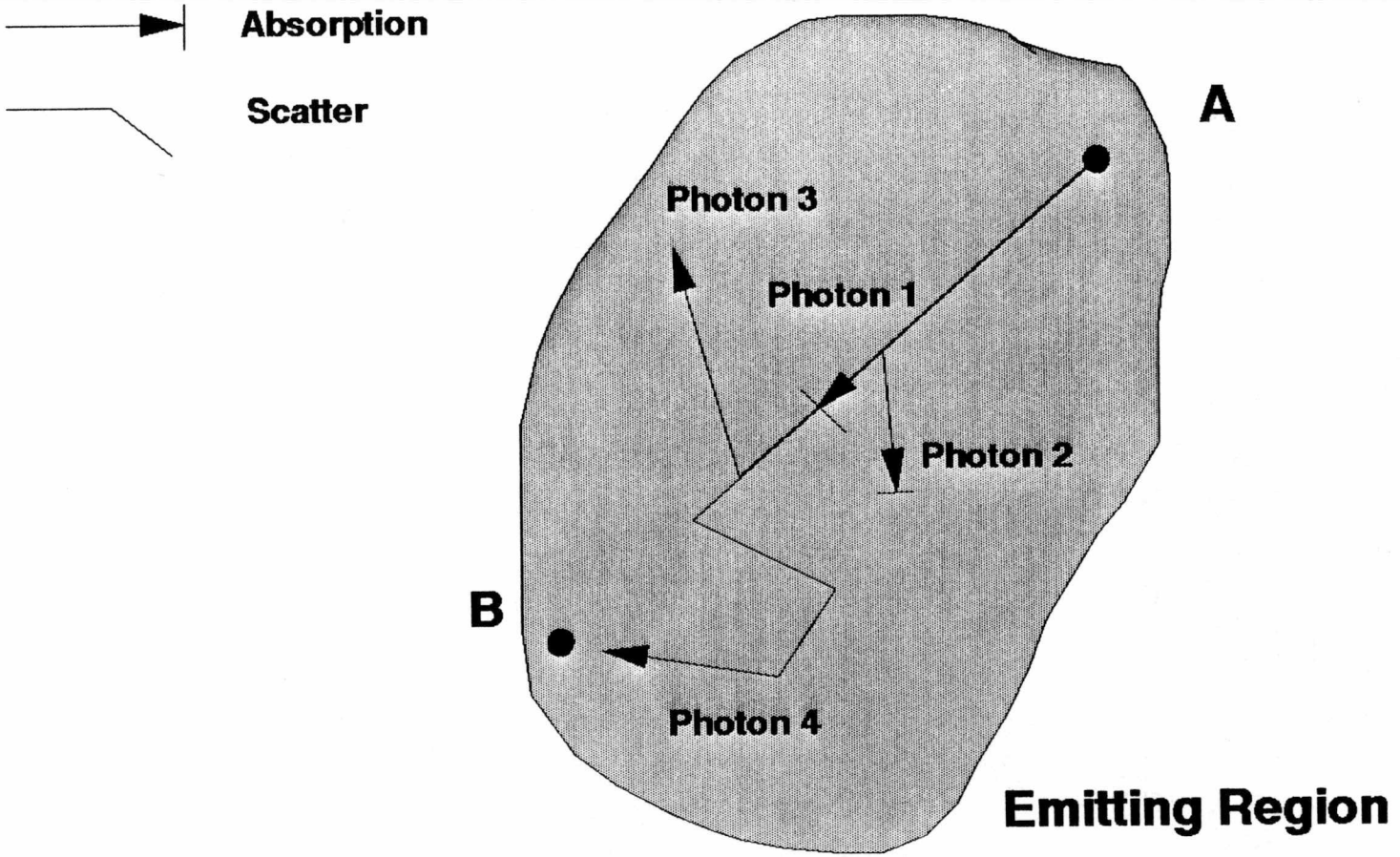


Figure 7. Some Possible Photon Paths.

different point A locations so that a volume integration over the media would result. It can be seen that much time is spent on calculating photon paths which never make it to point B.

A significant improvement in the efficiency of the Monte Carlo technique as applied to radiative heat transfer can be realized by utilizing the theory of reciprocity.[15,16] This theorem states that an equivalent process to that described above is to shoot photons from point B into the media; the volumetric emission phenomenon can be replaced by a path phenomenon. Although this is a nonphysical approach to the radiative transfer problem, significant computational advantages exist in using the reverse Monte Carlo procedure. In the reverse Monte Carlo procedure, by definition, calculations are performed only on those photons that arrive at point B. Thus, only those volumetric regions which are radiatively significant to the radiance at point B are identified.

## 7.2 Monte Carlo Radiative Transfer Code

The physical events which must be incorporated into the Monte Carlo radiative transfer code are absorption, scattering and selection of the scattering angle. The cumulative probability that a photon of a given frequency which traverses a given path length, $\delta s$, will encounter an interaction with the medium is related to the extinction cross-section of the path.

$$P_0 = 1 - e^{-\beta \delta s} \tag{7.1}$$

If an interaction occurs, the probabilities of absorption and scattering are defined by:

$$P_{abs} = (1 - \omega) \tag{7.2}$$

and

$$P_{scat} = \omega \tag{7.3}$$

In the limit of a purely scattering medium ($\omega = 1$), all photons are scattered and the probability for absorption $P_{abs}$ is zero. If an absorption event occurs, the determination of the absorber is related to the ratio of absorption cross-sections. That is, the probability that the absorption was caused by a particle is given by:

$$P_{part} = \frac{\sigma_{abs}}{k + \sigma_{abs}} \tag{7.4}$$

and likewise the probability that the absorption was caused by the gas is:

$$P_{gas} = (1 - P_{part}) \tag{7.5}$$

The Monte Carlo code used for the calculations presented utilizes the time reverse procedure described in Section 7.1. The simulation begins by traversing a photon along a small increment in path length, $\delta s$, along the initial line of sight direction. The transmission of this incremental path is determined and the interaction probability is determined using Equation (7.1). A random number between 0 and 1 is generated; if the random number is less than the transmission of the incremental path, no interaction of the photon and the path occurred, if the random number is greater than the path transmission, an interaction occurred and the location of the interaction is determined by drawing another random number and assuming that the location of the interaction is equally probable anywhere along the incremental path, $\delta s$. The substance of interaction can be determined by drawing another random number and using the value of the local scattering albedo (Equation (7.2) and Equation (7.3)). If the random number is less than the local scattering albedo, a scattering event has occurred, if not, then an absorption event has occurred. Identification of the absorber can be determined similarly, by drawing a random number and forming the

ratio of absorption cross-sections of the gas and particles. If a scattering event has occurred, the scattering angle is determined by drawing a random number and calculating the angle depending on this random number and the functional form of the scattering phase function. A new propagation direction is thus determined and the simulation is continued. All photons are tracked until they are either absorbed or exit the medium. The absorption of the medium is the ratio of absorbed photons to the total number of photons simulated. Since the Monte Carlo simulation is based on monochromatic properties of the medium, the emissivity is equivalent to the absorption.

## 7.3 Monte Carlo Solution for a Cylinder

The solution of the transfer equation using the method described in Section 7.2 is applied to a homogeneous cylindrical medium which is depicted in Figure 8. For this example, a set of properties which approximate the exhaust from the Space Shuttle Solid Rocket Booster (SRB) are used. The SRB propellant is a high performance composite propellant grain which has a 19% aluminum mass loading. The exhaust of the SRB is approximated by a homogeneous cylinder with a 1.9 m radius and 60 m in length. The temperature, pressure and mole fractions of $H_2O$ and $CO_2$ were taken from the One Dimensional Equilibrium (ODE) nozzle exit plane code calculations of Reference 17. These properties predicted for sea level operation are summarized in Table 1. Aluminum oxide particles are assumed to be present in the exhaust. The particle radius is assumed to be 5.8-μm based on the Hermsen particle size correlation.[18] The aluminum oxide mass fraction at the exit plane is approximately 28% which corresponds to a particle number density on the order of 10,000 particles/cm$^3$. The particle optical properties were taken from Reference 19. For this case, the particle albedo was set to 1 (conservative scattering)

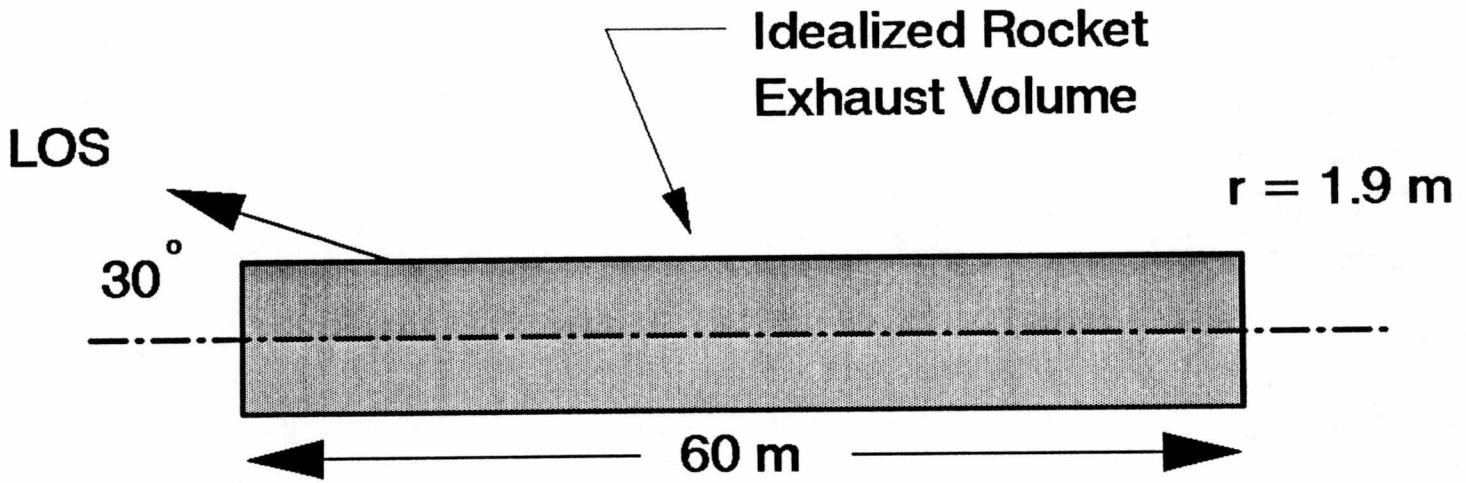


Figure 8. Base Heating Geometry.

Table 1. Summary of Solid Rocket Booster Exhaust Properties.[17]

| **Property** | **Chamber** | **Nozzle Exit Plane** |
|---|---|---|
| Pressure, atm | 54.44 | 1.178 |
| Temperature, K | 3406 | 2276 |
| Exit Area Ratio | - | 7.72 |
| $Al_2O_3$, mole Fraction | 0.07442 | 0.07985 |
| $H_2O$, mole Fraction | 0.1414 | 0.1406 |
| $CO_2$, mole Fraction | 0.01609 | 0.01249 |

or totally scattering particles. A forward-looking line of sight inclined 30° to the thrust axis, and intersecting the axis two nozzle exit radii downstream of the nozzle exit plane was chosen for these predictions. Shown in Figure 9 are the particle absorption and scattering cross-sections for this test case, along with the 5 $cm^{-1}$ averaged gas absorption coefficient band model parameters which are taken from Reference 20.

The results of the Monte Carlo simulation for the base heating scenario are shown in Figure 10. Shown is the emissivity of the medium as a function of gaseous absorption coefficient. This solution assumes conservative scattering with all absorption attributable to the gas. Atmospheric effects (emission/attenuation) are neglected. The data in the figure show that at small gaseous absorption coefficient values, where the probability of scattering is large compared to that of absorption, the emissivity is small. As the gaseous absorption coefficient is increased, the probability for absorption increases and thus the emissivity increases. The medium becomes black as the probability of absorption becomes very large compared to the scattering probability and most photons are absorbed upon the first interaction with the medium. As a check on the Monte Carlo results, the analytic solution for the case of no scattering is also plotted on Figure 10. The convergence of the Monte Carlo simulation for a gaseous absorption coefficient of 0.01 $cm^{-1}$ is shown in Figure 11. The emissivity is shown as a function of the number of photons simulated. The variation in emissivity above approximately 4000 photons simulated is not great, at least for this absorption coefficient, and a sample size of 20,000 photons is not required to achieve convergence.

Since the Monte Carlo process consists of repeated trials with ultimately only two possible outcomes (the photon is either absorbed or transmitted), and since each new trial is independent and the probability of absorption or transmission remain constant, the process may be referred to as a Bernoulli process.[21] The standard deviation of the

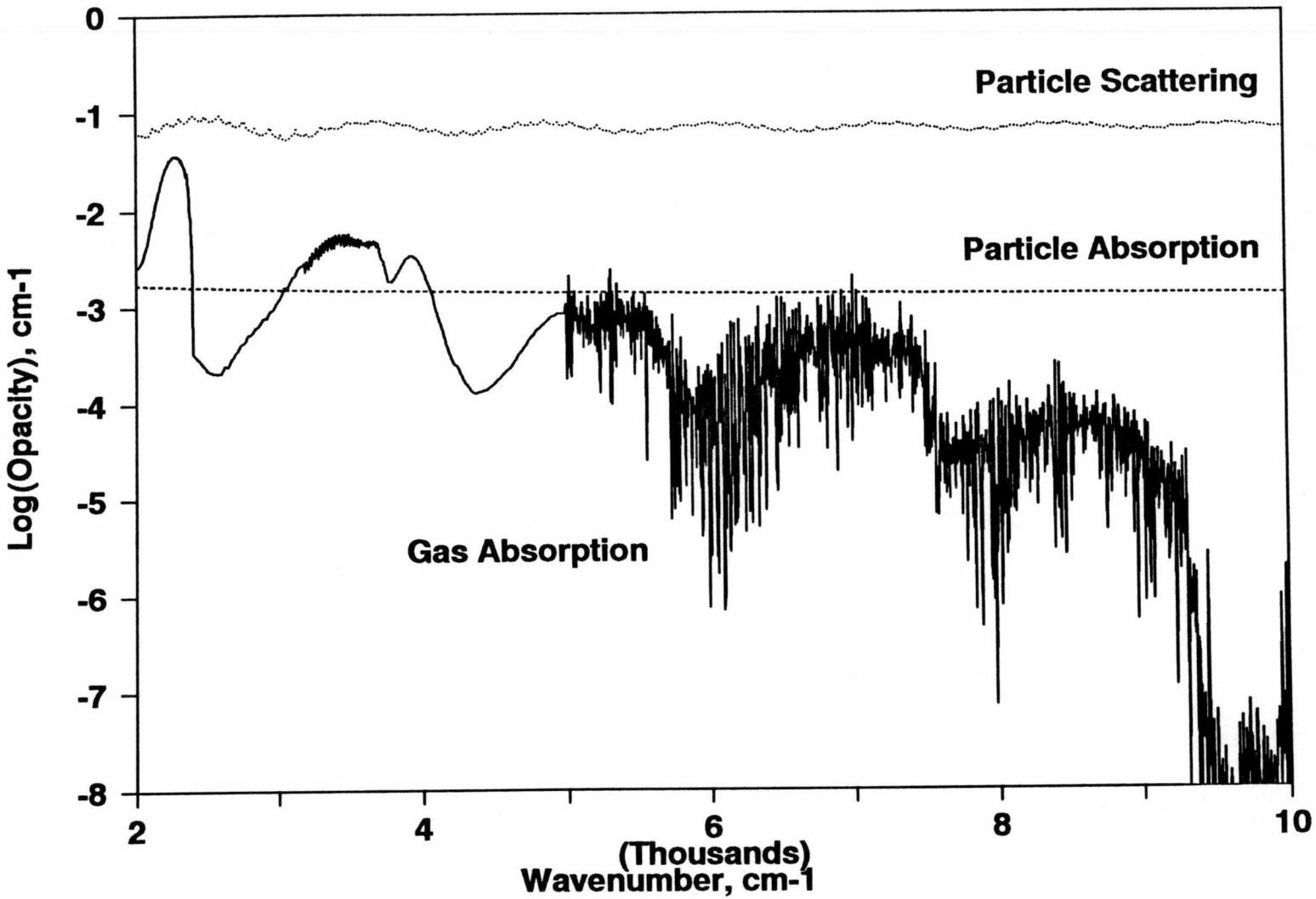


Figure 9. Test Case Opacity Contributions.

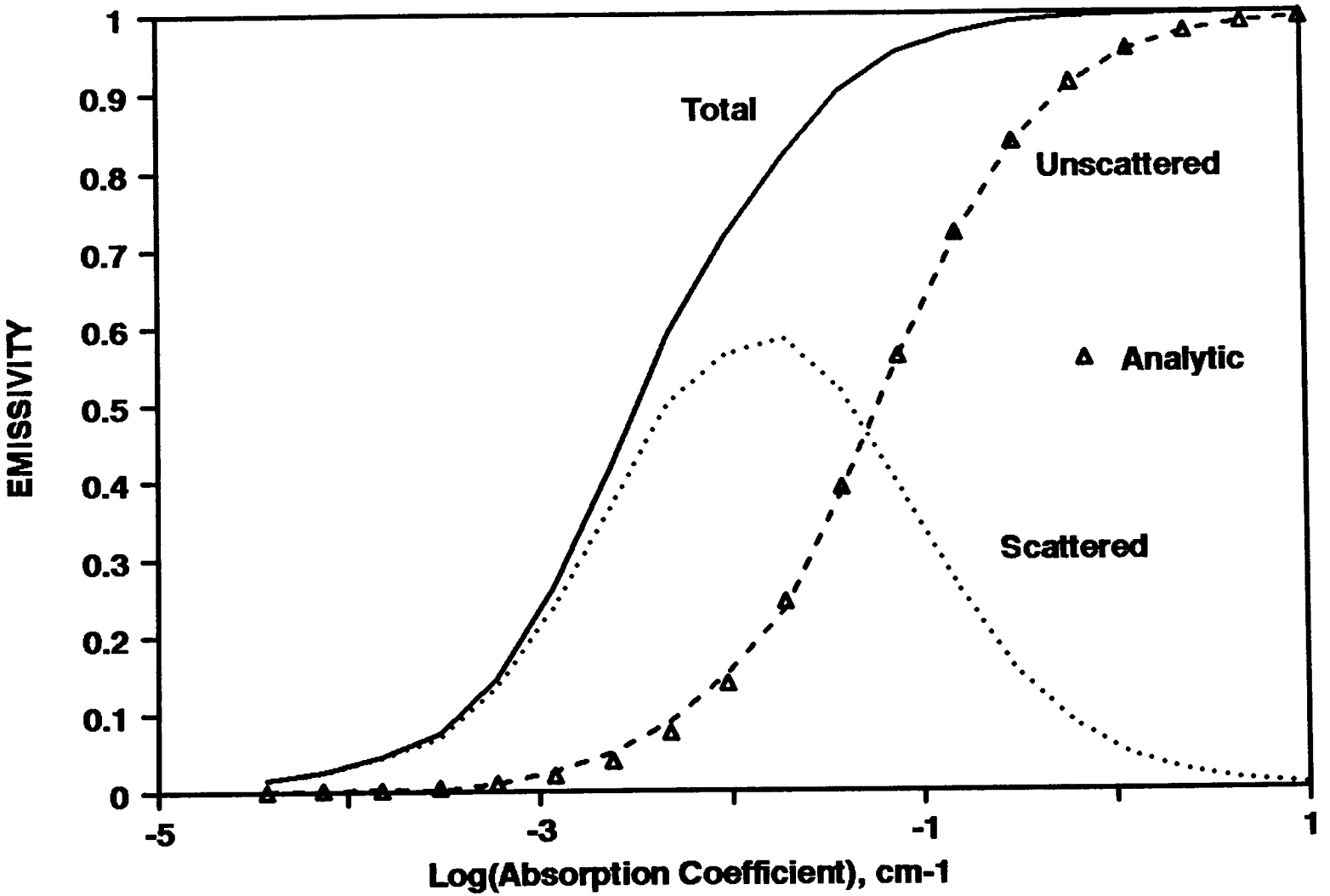


Figure 10. Base Heating Test Case Solution.

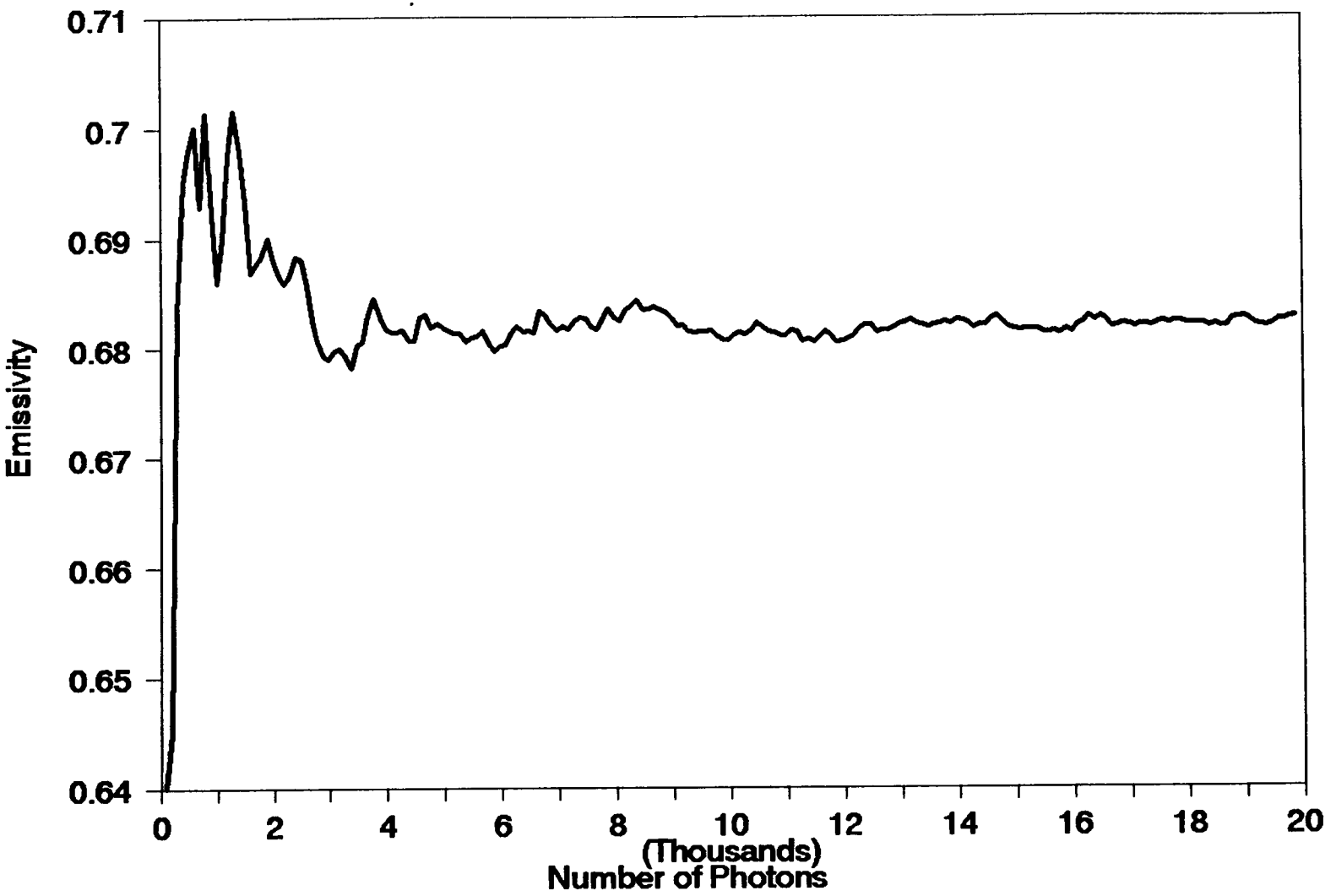


Figure 11. Convergence of Monte Carlo Simulation.

emissivity determined from the Monte Carlo calculations shown in Figure 10 may be estimated by assuming a binomial probability distribution. The standard deviation of the emissivity of the medium is:

$$\sigma_\varepsilon = \sqrt{\frac{\varepsilon\tau}{N}} \tag{7.6}$$

where

$\sigma_\varepsilon$ is the standard deviation of the emissivity

$\varepsilon$ is the emissivity

$\tau$ is the transmissivity

N is the total number of trials or photons

The standard deviation of the total emissivity calculations shown in Figure 10, as estimated by Equation (7.6), is shown in Figure 12.

The emission from a scattering medium can be written as a sum of emission components from various scattering orders or the number of times that a photon has encountered a scattering event before it reaches the observer or the base region. This is represented by Equation (2.2) where the emissivity is the sum of the unscattered emission and the scattered emission. This is illustrated for the base heating problem in Figure 12. The gaseous absorption coefficient is $0.01 cm^{-1}$ and the emissivity component for each scattering order group is shown in Figure 13. The importance of multiple scattering is evident by the significant contribution to the emissivity from scattering orders as high as 15. The sum of the emissivities for all of these groups is the total emissivity for the line of sight. For this case, the total emissivity is 0.68.

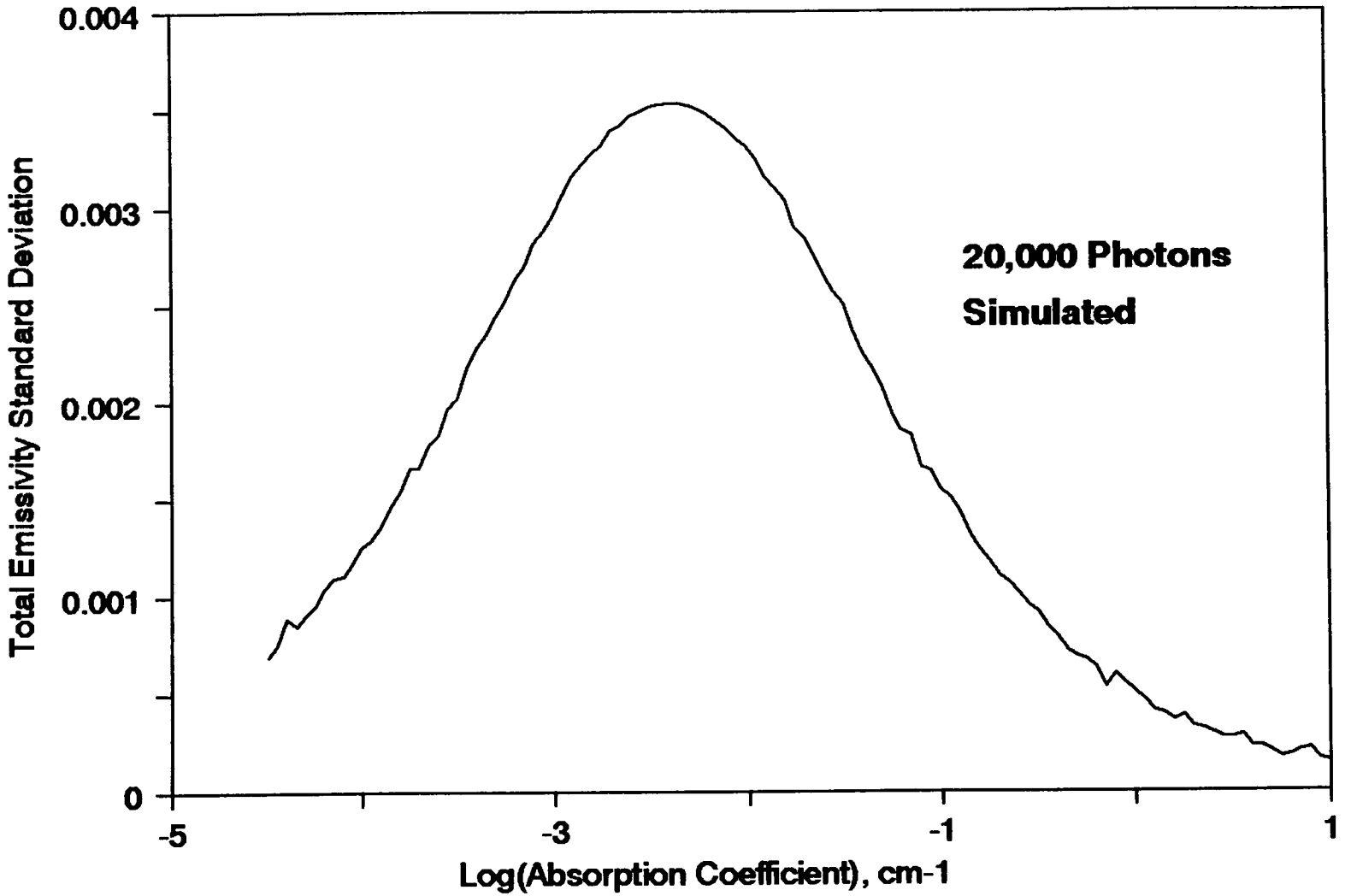


Figure 12. Monte Carlo Total Emissivity Standard Deviation Estimate.

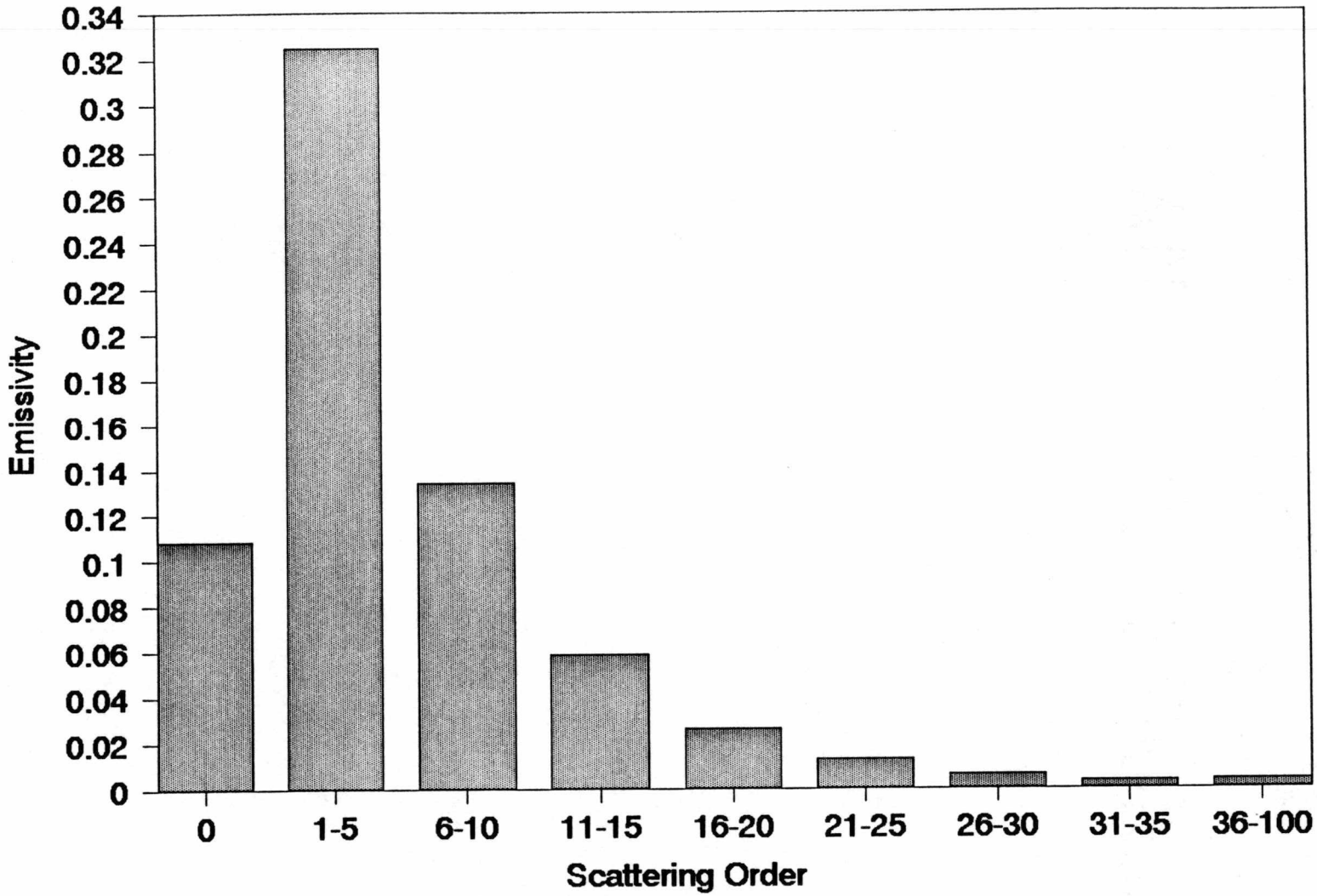


Figure 13. Contributions of Scattering Orders to the Total Emissivity.

## 7.4 Monte Carlo Code Performance

The Monte Carlo radiative transfer code was written in FORTRAN compiled with a 32 bit compiler, and run on an IBM compatible personal computer (PC) with a 33 MHz Intel 80486 processor. The results shown in Figure 10 required approximately 6 hours. on the PC to produce. Run times are highly dependent on several factors, including the number of photons simulated and the specific geometry and properties of the simulation. Typically, 20,000 photon paths at a given gaseous absorption coefficient were computed for the calculations reported herein. The time required for simulation depends on how far each individual photon must be tracked until it is either absorbed, or exits the media. For the cases of low absorption coefficient, where scattering is dominant, the photon paths are very long and the simulation time required for each photon is very large (up to 1 sec per photon). Where absorption dominates however, photons encounter absorption within a relatively few or no scattering events and thus the simulation time is very fast. The results shown in Figure 10 are for only one line of sight from the exhaust to the body. A complete heat transfer calculation for the base heating situation would involve the calculation of many lines of sight and would quickly become impractical on a PC-class computer.

## 8.0 BAND MODEL TREATMENT OF SCATTERING

In order to incorporate the Monte Carlo simulation results, such as those shown in Figure 10, into a band-model formulation, the absorption coefficient probability distribution function for a particular band model must be determined. Then the proper band model averaging of the monochromatic solutions to the scattering transport equation may be determined by integration over frequency, or over the absorption coefficient probability distribution:

$$\bar{g} = \frac{1}{\delta v}\int_{\delta v} g(v)dv = \int_0^\infty g(k)f(k)dk \tag{8.1}$$

where g is the spectrally averaged quantity and f(k) is the absorption coefficient probability. Integration of the emission spectrum over frequency is by far the most straightforward technique to obtain the spectrally averaged emission. However, when using a random band model, a statistical description of spectral structure of the band is all that is known. Therefore integration over an absorption coefficient probability distribution is the most readily applied method.

The expression for the probability of an absorption coefficient within a spectral band for a particular band model can be determined from the band model parameters.[22] For an "exponential tailed 1/S" distribution of line strengths[23], the line strength distribution function is given by:

$$P(S) \propto \frac{1}{S} e^{-\frac{S}{\pi S_0}} \tag{8.2}$$

and the corresponding expression for the absorption coefficient probability for Lorentz

broadened lines is given by:[22]

$$f(k) = \sqrt{\frac{\bar{k}_{\delta\nu}\alpha}{\pi k^3}} \exp\left[\alpha\left(2 - \frac{\bar{k}_{\delta\nu}}{k} - \frac{k}{\bar{k}_{\delta\nu}}\right)\right] \tag{8.3}$$

The mathematically correct, band-model-averaging treatment of the scattering problem can now be performed using Equations (8.1) and (8.3) and Monte Carlo simulation results, such as those presented in Figure 10.

# 9.0 EVALUATION OF APPROXIMATE METHODS (RESULTS)

Three approximate solution methods to the band model scattering problem are evaluated against the mathematically correct solution. The approximations are: the "hybrid" band model, the two flux scattering approximation and emission averaging. Each of these approximations will be described and applied to the finite cylinder base heating problem shown in Figure 8.

## 9.1 Hybrid Band Model Approximation

For a band treatment of a gaseous emission spectra, only band-averaged spectral properties of the gas are known; that is, the band-averaged gaseous emissive properties. Therefore, information about the spectral absorption coefficient for the gas which is needed to solve the monochromatic transport equation is not available. The hybrid band model approximation performs a correct band model spectral average for the unscattered emissivity (one dimensional) but evaluates the scattered (three dimensional) emissivity using Beer's law with the spectral band averaged gas absorption coefficient. That is the unscattered radiative transfer from the gas is treated correctly using a gaseous band model, but the scattered radiation is treated using Beer's Law.

$$\bar{\varepsilon}_{\delta\nu} = \bar{\varepsilon}_{unscattered}(k) + \varepsilon_{scattered}(\bar{k}) \tag{9.1}$$

The hybrid band model approximation is used implicitly in any band model scattering formulation. This approximation has the advantage of approaching the result for pure gas in the no scattering limit and that it can be applied to realistic inhomogeneous media. For

this example, the hybrid model uses the full three-dimensional scattering phase function so any error can be attributed to the improper averaging of the scattered radiance term in Equation (9.1).

The hybrid band model may be computed using Equation (8.1), Equation (8.3) and the Monte Carlo calculations shown in Figure 10. A FORTRAN program was written to perform the integration shown in Equation (8.1) using Simpsons rule. Performing this integration required approximately 5 minutes on the computer system described in Section 7.4. The results of the approximation and the mathematically correct solution for the base heating problem are shown in Figure 14. The total time required to produce the prediction shown in Figure 14 is approximately 6 hours. This is in sharp contrast to the estimated 5 minutes that would be required to perform the calculations if an approximate band model scattering formulation were used. As can be seen the hybrid approximation does a good job in the weak absorption portions of the spectra, but a relatively poor job near the center of the band at 2.7-μm the hybrid band model over predicts the emission by approximately 30% in the 2-μm to 5-μm wavelength band.

The fundamental flaw in the hybrid band model approach for this base heating scenario is revealed by examining its curve of growth which is shown in Figure 15. Although the hybrid band model curve of growth behaves correctly in the optically thin and thick limits, it fails to increase monotonically with increasing opacity.

## 9.2 Two-Flux Approximation

The two-flux approximation replaces the three dimensional scattering function with two delta functions, one in the forward (0°.) direction and one in the backwards (180°.) direction. This approximation is also called the Schuster-Scharzchild

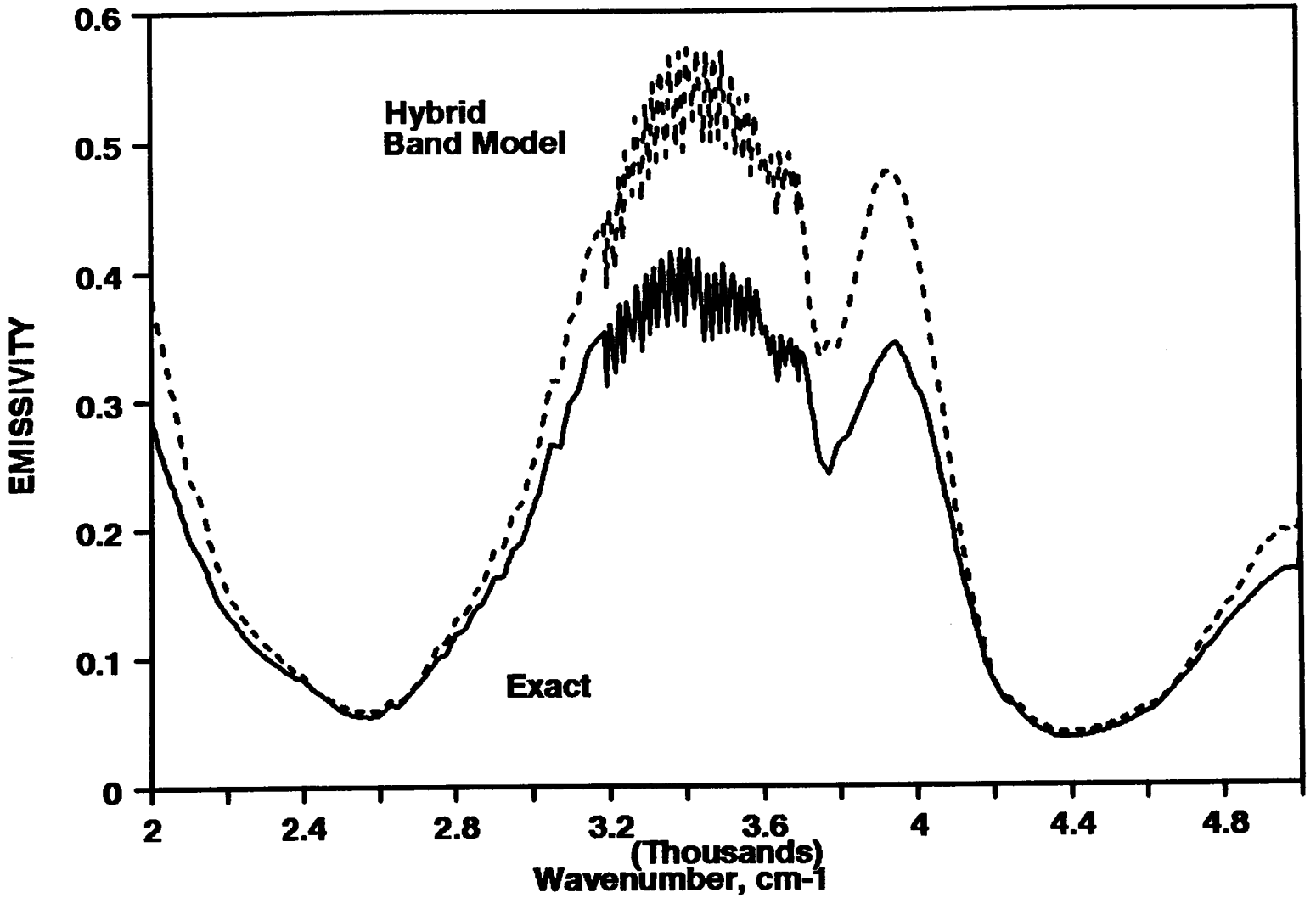


Figure 14. Exact versus Hybrid Band Solution.

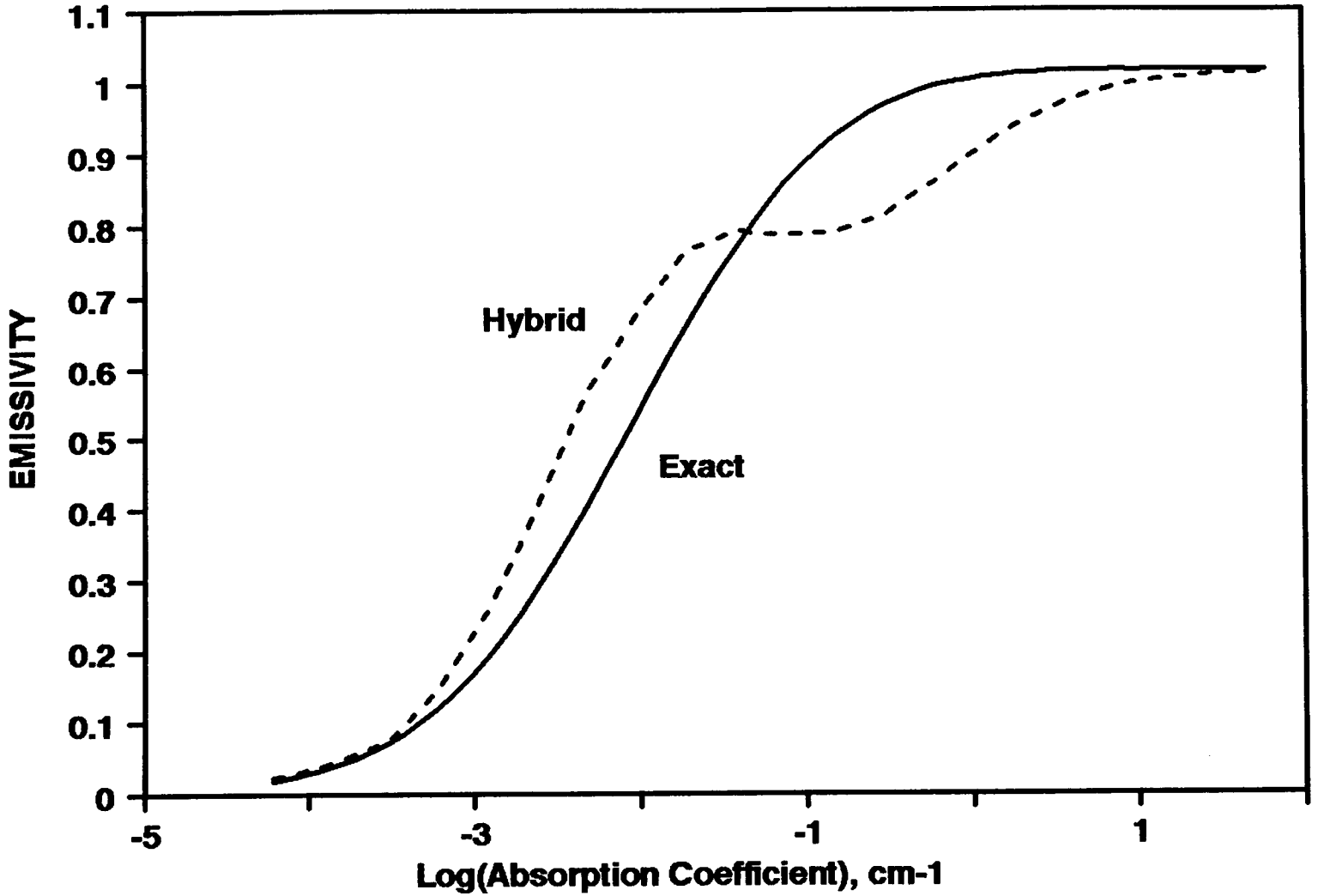


Figure 15. Hybrid Band Model Curve of Growth.

approximation.[7] The monochromatic two-flux emissivity is a simple analytic expression.[24] This expression is extended to a band model result by spectrally averaging in the transform domain according to Equation (9.1). The value of the backscatter fraction b was chosen as 0.3 based on the 0.7 asymmetry factor of the Henyey-Greenstein scattering phase function. The error in the two-flux approximation is basically attributed to the one-dimensional nature of the approximation. The results of the approximation plotted against the correct three dimensional solution is shown in Figure 16. The calculations shown in Figure 16 required approximately 5 hours to perform using the computer system described in Section 7.4. The two-flux approximation does well at the center of the band where the absorption is high but relatively poorly in the wings where scattering dominates and the one dimensional approximation to the true three dimensional process is most important.

For the small aspect angles typical of base heating, use of the two-flux approximation can lead to large errors in the predicted emission from the exhaust gas. This is due to the restriction that scattering occurs only in the forward or backward directions. Photons emitted towards the body that would normally scatter away from the body in the correct three-dimensional scattering phase function are artificially forced to retain their original propagation direction. Shown in Figure 17 is the emissivity of a cylinder with an infinite length, radius of 50 cm, an optical depth based on the diameter of 20, and is composed of a highly scattering media with an albedo of 0.9, as a function of the viewing aspect angle. An aspect angle of 0° corresponds to the grazing angle, and 90° corresponds to side on. The two-flux calculation shows that the emission is independent of aspect angle. The correct three dimensional treatment, using an isotropic scattering phase function of the same problem, shows significantly different results.

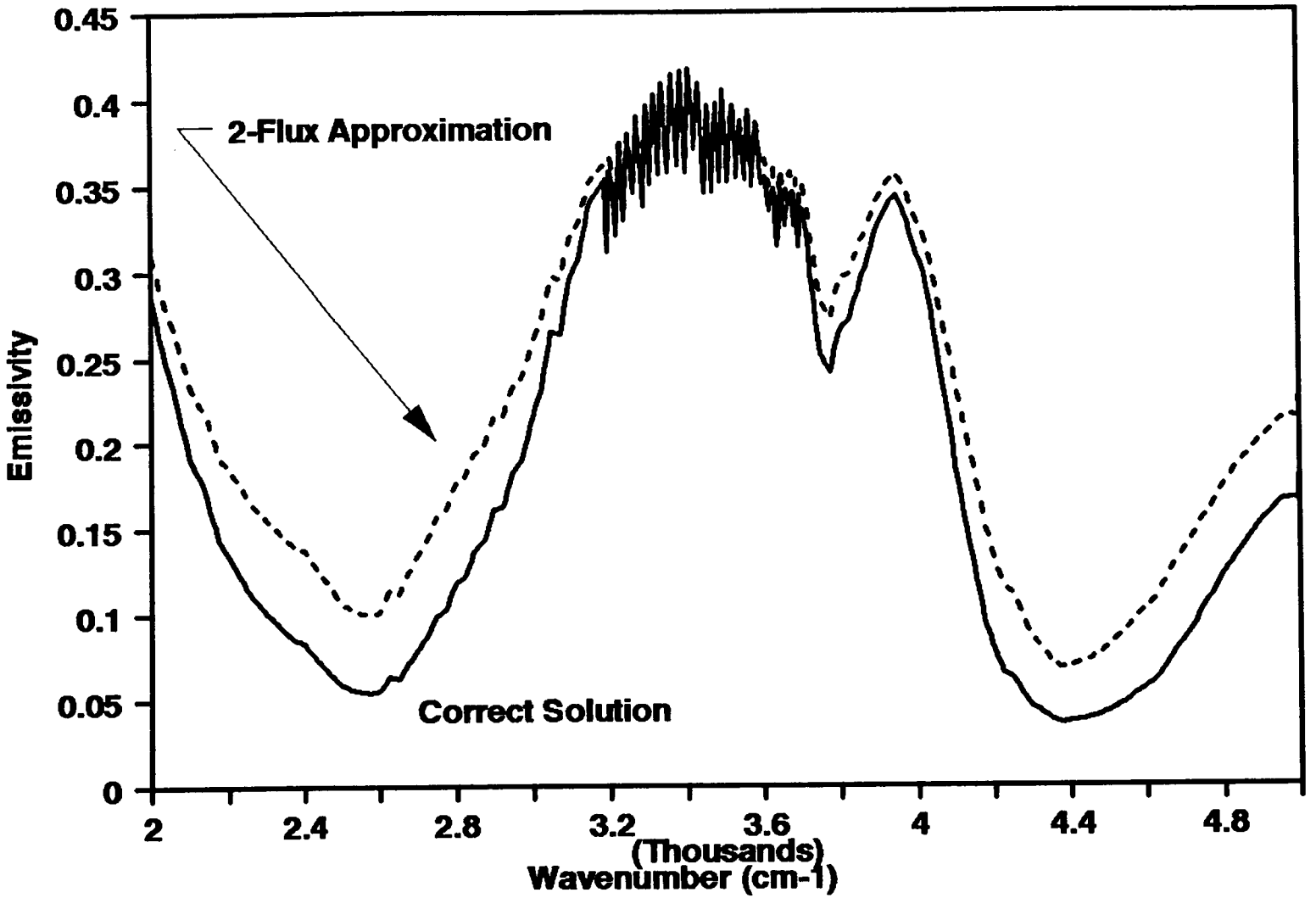


Figure 16. Exact and Two-Flux Approximation Comparison.

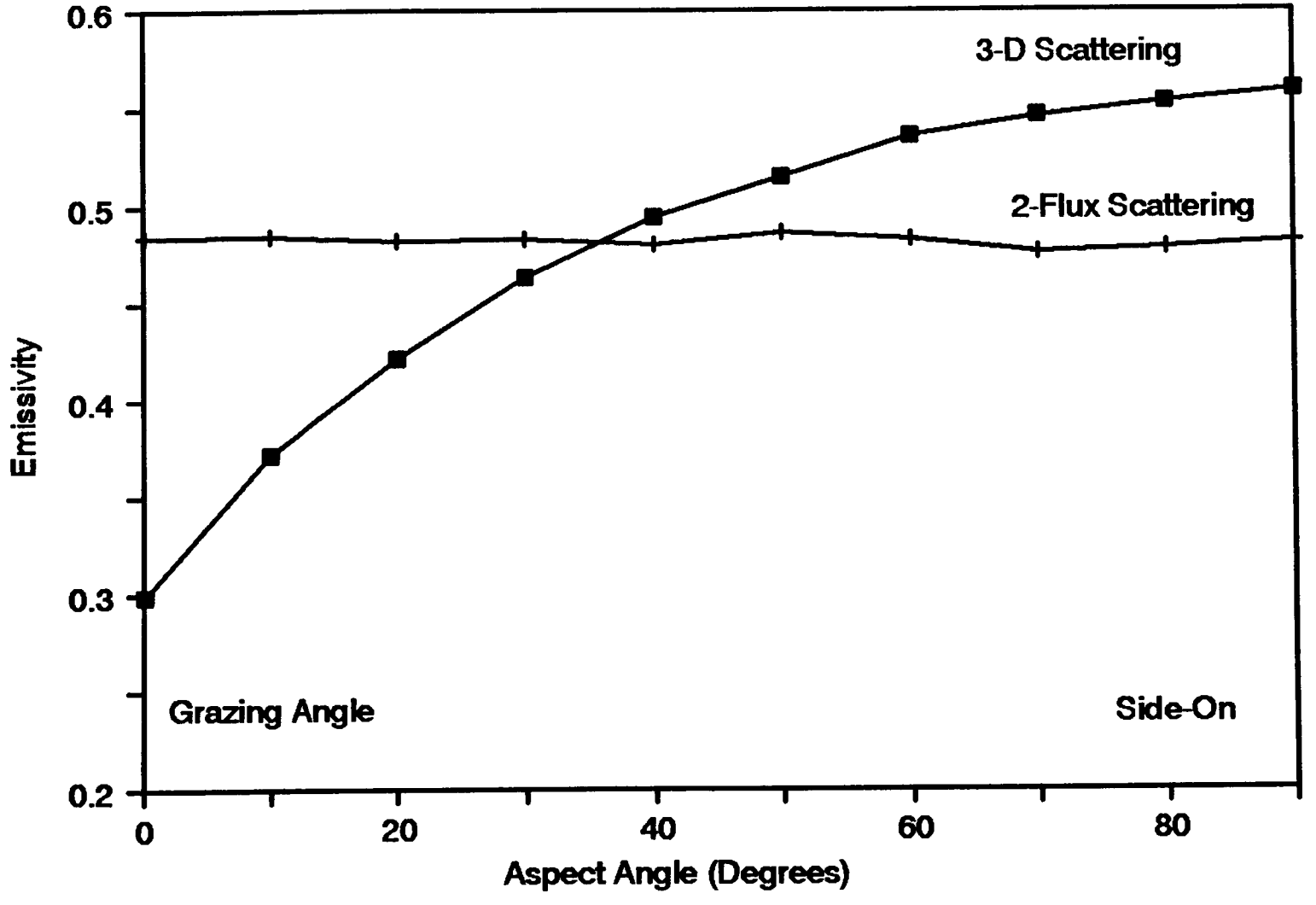


Figure 17. Two-Flux Aspect Angle Problem for an Infinite Cylinder.

## 9.3 Emission Averaging

When the particles and gas in a media exist at different temperatures, as is often the case in solid propellant rocket exhausts, the source function in the radiative transport equation (Equation (5.3)) becomes:

$$S_\nu(s) = \frac{k_\nu}{\beta_\nu} I_{b\nu}(T_{gas}) + \frac{\sigma_a}{\beta_\nu} I_{b\nu}(T_{part}) + \omega_\nu \int_{4\pi} P(\Omega' \cdot \Omega) I_\nu(s, \Omega') d\Omega' \qquad (9.2)$$

An approximation is often used where an effective emission function is formulated by performing a weighted average of the gas and particle emission terms.[17] The proper emission averaging would be performed on a spectral basis, however, since only spectrally averaged band model parameters are known, the following equation is used:

$$\bar{I}_{b_{eff}} = \frac{\bar{k}_{gas}}{\bar{k}_{gas} + \sigma_a} I_b(T_{gas}) + \frac{\sigma_a}{\bar{k}_{gas} + \sigma_a} I_b(T_{part}) \qquad (9.3)$$

where $\bar{k}_{gas}$ is the band averaged gaseous absorption coefficient and $\sigma_a$ is the particle extinction coefficient and $\bar{I}_{b_{eff}}$ is an equivalent, emission averaged Planck function. Spectral averages are not shown on the Planck function and the particle properties due to the spectral invariance of these over the typical spectral intervals of a band model. This expression replaces the Planck function in the transport equation source function (Equation (5.1)). This approximation can be extended to any number of particle groups not in thermal equilibrium with the gas. A mathematically correct solution to this problem can be obtained using the Monte Carlo procedure previously described with one additional step. Upon absorption, the probability of absorption by the gas is given by:

$$P_{gas} = \frac{\bar{k}_{gas}}{\bar{k}_{gas} + \sigma_e}$$

The probability of absorption by a particle is $(1 - P_{gas})$. The resulting emission at the point of interest is given by:

$$I_{Total} = P_{gas} I_b(T_{gas}) + P_{part} I_b(T_{part})$$

The results of this analysis and approximation are shown in Figure 18 which shows the emission spectrum of the rocket exhaust model for both the mathematically correct treatment and the approximate emission-averaging treatment. The approximation does well in the weak gas emission regions but less well near the band center. These calculations required approximately 6 hours to perform using the computer system described in Section 7.4. Shown in Figure 19 is the percentage error introduced by using the averaged source function in the place of the full source function as a function of the ratio of the particle absorption cross-section to the total absorption cross-section, $\Gamma$, where $\Gamma$ is given by:

$$\Gamma = \frac{\sigma_a}{\sigma_a + \bar{k}}$$

The approximation converges to the exact formulation in the limits of particle albedo approaching 0 and 1 and shows a maximum error introduced by the approximation for the base heating test case of less than 7%.

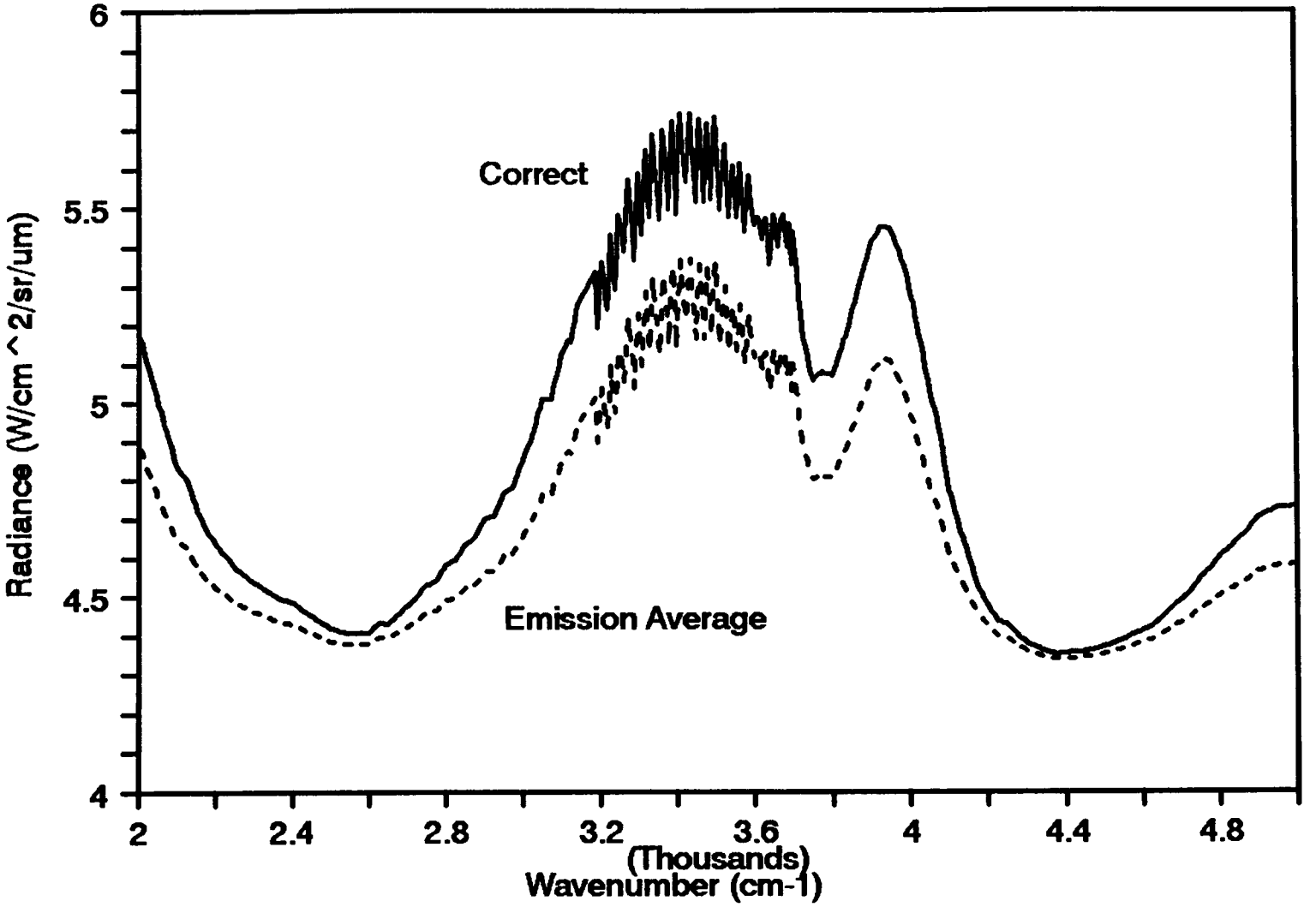


Figure 18. Emission Averaging Approximation Spectrum.

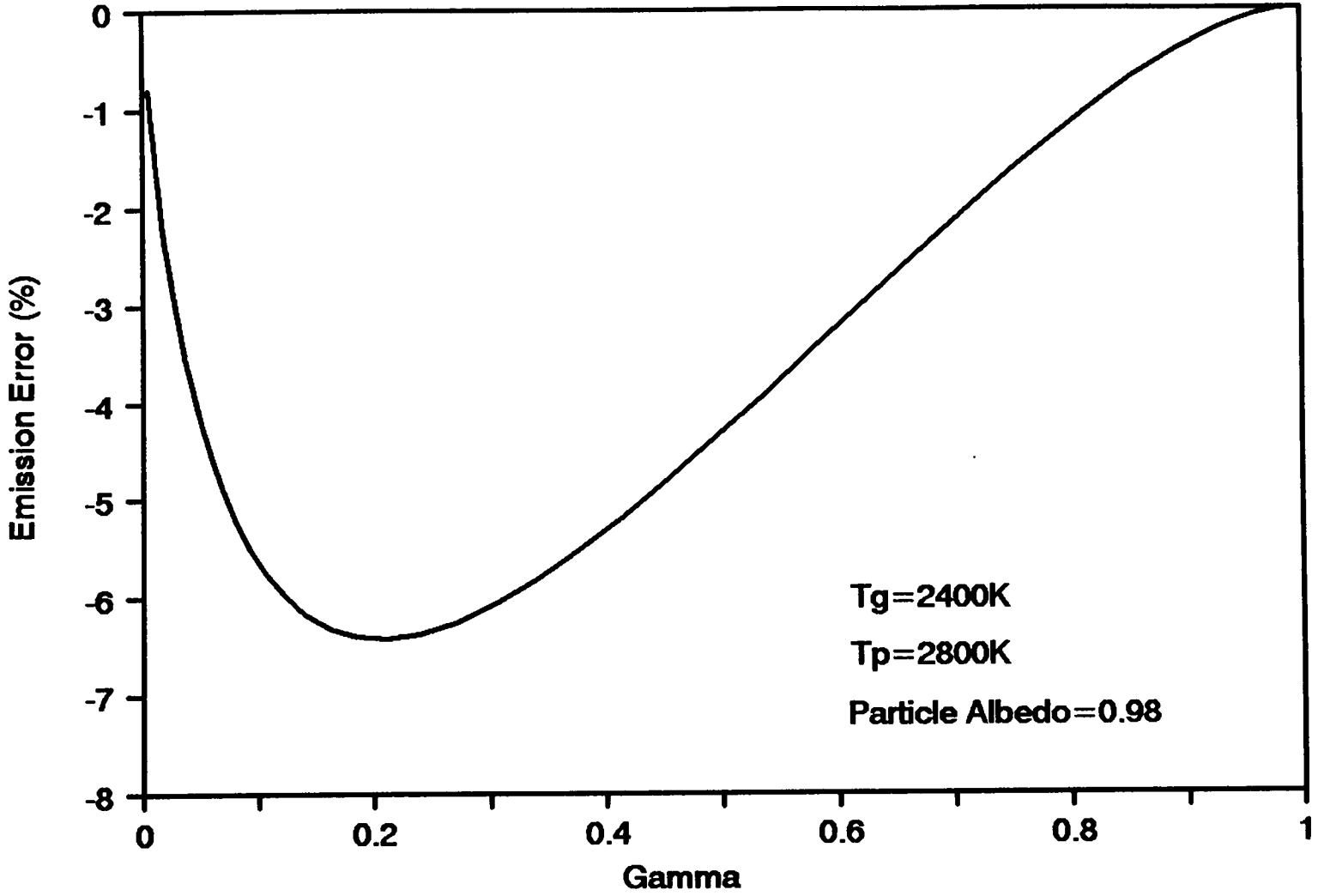


Figure 19. Base Heating Emission Averaging Error.

# 10.0 DISCUSSION OF RESULTS

A method to generate mathematically correct solutions to the radiative transport equation for an emitting and scattering medium has been developed. These solutions can then be passed through an averaging procedure by which a band model solution can be produced. This mathematically correct band-averaged solution can then be compared with an approximate solution method to determine the efficacy of the approximation for the particular situation of interest. Three approximate solution techniques have been examined for a representative base heating scenario. The first approximation examined is called the hybrid band model where the correct band averaging is performed on the unscattered transport terms, and Beer's law is used on the scattered terms. This approximation is implicit in all scattering band model calculations. The hybrid band model approximation performed best in the weak gas spectral regions but produced a nonphysical curve of growth. For the base heating scenario examined, use of a band model scattering treatment will result in a 30% overprediction in the emission in the 2 to 5-μm spectral region, solely due to the mathematical error introduced by the scattering band model. The second approximation uses a one-dimensional approximation to the scattering phase function where photons are allowed to scatter only along the line of sight. This approximation is exact in its spectral nature, that is the band averages are performed correctly, but is approximate in the spatial resolution of the problem in that a one-dimensional scattering phase function is used. This approximation is often viewed as a relatively fast running, good approximation to a full three dimensional scattering treatment. The two-flux approximation performed best in the strong absorption gas spectral bands where the majority of the energy is emitted. Since the two-flux approach did well in the strong

emission spectral regions for the base heating scenario, this does seem to be a reasonable alternative to a more computationally expensive three-dimensional scattering treatment. The third approximation examined, emission averaging, is often applied for the situation where the gas and particles in a rocket exhaust are at different temperatures. This approximation has a maximum emission error of 7% for the base heating scenario examined. Compared to the error introduced by the scattering band model treatment (the hybrid band model), the error introduced by emission averaging the source term is small and for the present time deemed acceptable.

The computer runtimes required to produce the results reported in this work reflect the high computational cost required for a rigorous treatment of the scattering problem. Approximate treatments used for engineering calculations, which often make use of all three of the approximations discussed in this work, require at least an order of magnitude less computing time than the Monte Carlo routines used in this work.

# 11.0 SUMMARY AND RECOMMENDATIONS

A mathematically correct solution to the band model scattering problem has been developed and demonstrated for an idealized homogeneous representation of a rocket motor exhaust. Application of this technique to a inhomogeneous medium and to a medium which contains a particle size distribution would extend the utility of this procedure to more realistic rocket motor exhaust models. This extension would require modification of the Monte Carlo code such that the probabilities for photon absorption and scattering would be based on the local properties of the medium, instead of constant values.

The uncertainties involved in making a radiative heating prediction from a combustion exhaust source are dominated by uncertainties in predicting the physical properties of the gaseous species in the flow, such as the temperature, pressure, species concentrations, radiative properties, and the properties of the particulates such as temperature, size distribution and optical properties. Therefore, until the state of the art in predicting or measuring these quantities improves, errors introduced by the approximate radiative transfer equation solution techniques shown in this work will be overshadowed.

# LIST OF REFERENCES

## LIST OF REFERENCES


(1) Ludwig, C. B., Handbook of Infrared Radiation from Combustion Gasses, NASA SP-3080, 1973.

(2) Malkmus, W., "Some Comments on the Extension of Band Models to Include Scattering," *J. Quant. Spectroscopy and Radiative Transfer*, Vol. 40, Sept. 1988, pp. 201-204.

(3) Rothman, L. S., "The HITRAN Database: 1986 Edition," *Applied Optics*, Vol. 26, Oct. 1987, p. 4058.

(4) Sutton, G. P., Rocket Propulsion Elements, Sixth Edition, Wiley, New York, 1992.

(5) Hill, P. G., and Peterson, C. R., Mechanics and Thermodynamics of Propulsion, Addison-Wesley, 1970.

(6) Rao, G. V. R., "Recent Developments in Rocket Nozzle Configurations," *J. Amer. Rocket Soc.*, 31, 11, Nov. 1961, pp. 1488-1494.

(7) Özisik, M. N., Radiative Transfer and Interactions with Conduction and Convection, Wiley, 1973.

(8) Van de Hulst, H. C., Multiple Light Scattering: Tables, Formulas, and Applications, Academic Press, New York, 1980.

(9) Goody, R. M., Atmospheric Radiation, Oxford University Press, 1964.

(10) Plass, G. N., "Models for Spectral Band Absorption," *J. Opt. Soc. of Am.*, Vol. 48, No. 10, Oct. 1958, pp. 690-703.

(11) Ladenberg, R., and Reiche, F., *Ann. Physik*, 42, 181,1913.

(12) Erdélyi, A., et al., *Tables of Integral Transforms*, McGraw-Hill, 1954, Vol. I, p.195.

(13) Young, S. J., "Band Model Calculations of Atmospheric Transmittance for Hot Gas Line Emission Sources," SAMSO-TR-74-248, 1974.

(14) Arfkin, G., Mathematical Methods for Physicists, Academic Press, 1970.

(15) Marchuk, G. I., The Monte Carlo Methods in Atmospheric Optics, Springer-Verlag, 1980.

(16) Walters, D. V., and Buckius, R. O., "Rigorous Development for Radiation Heat Transfer in Nonhomogeneous Absorbing, Emitting and Scattering Media", *Int. J. Heat and Mass Transfer*, Vol. 35, No. 12, 1992, pp. 3323-3333.

(17) Pearce, B. E., "Predictions and Measurements of Radiation Base Heating from a Solid Rocket Motor Plume," AIAA-91-1431, AIAA 26th Thermophysics Conf., June, 1991.

(18) Hermsen, R. W., "Aluminum Oxide Particle Size for Solid Rocket Motor Performance Prediction," *AIAA J. Spacecraft and Rockets*, Vol. 18, No. 6, Nov.-Dec. 1981, pp. 483-490.

(19) Reed, R. A., and Calia, V., "Review of Aluminum Oxide Rocket Exhaust Particles," AIAA-93-2819, AIAA 28th Thermophysics Meeting, Orlando, FL., July 1993.

(20) Bernstein, L., S. Robersun, D. C., and Conant, J. A., "Band Model Parameters for the 4.3-μm $CO_2$ Band from 200 to 3000K," *Journal of Quantitative Spectroscopy and Radiative Transfer*, Vol. 23, 1980, pp. 169-185.

(21) Walpole, R. E., and Myers, R. H., Probability and Statistics for Engineers and Scientists, Fourth Edition, Macmillian Publishing Company, 1989.

(22) Domoto, G. A., "Frequency Integration for Radiative Transfer Problems Involving Homogeneous Non-Gray Gasses: The Inverse Transmission Function," *J. Quant. Spectroscopy and Radiative Transfer*, Vol. 14, 1974, pp. 935-942.

(23) Malkmus, W., "Random Lorentz Band Model with Exponential-Tailed $S^{-1}$ Line Intensity Distribution," *J. Opt. Soc. Am.*, Vol. 57, No. 3, 1967, pp. 323-239.

(24) Bartky, C. D., and Bauer, E., "Predicting the Emittance of a Homogeneous Plume Containing Alumina Particles," *AIAA J. Spacecraft*, Vol. 3, No. 10, Oct. 1966, pp. 1523-1527.

# VITA

Daniel Gaines Brown was born in Atlanta, Georgia on March 29, 1963. He graduated from North Gwinnett High School in June 1981. He attended Gainesville Junior College and the Georgia Institute of Technology, earning a Bachelors in Aerospace Engineering from the latter in 1985. He is married to Cynthia Nancy Holcomb Brown of Manchester, Tennessee.